AFRL-SR-BL-TR-98-

0142

REPORT DOCUMENTATION PAGE

1. AGENCY USE ONLY (Leave blank)	2. REPORT DATE	3. REPORT TYPE AND DATES COVERED
	1/98	Final 01 Apr 95 - 30 Nov 97

4. TITLE AND SUBTITLE Experimental Studies of Laminar, Transitional, and Turbulent Hypersonic Flows Over Elliptic Cones at Angles of Attack

5. FUNDING NUMBERS

G F 49620-95-1-0292

6. AUTHOR(S)

Michael S. Holden

7. PERFORMING ORGANIZATION NAME(S) AND ADDRESS(ES)

Calspan-UB Research Center (CUBRC)
4455 Genesee Street, P.O. Box 400
Buffalo, NY 14225

8. PERFORMING ORGANIZATION REPORT NUMBER

2650F

9. SPONSORING/MONITORING AGENCY NAME(S) AND ADDRESS(ES)

Air Force Office of Scientific Research
110 Duncan Avenue, Room B115
Bolling AFB, DC 20332-8050

NA

10. SPONSORING/MONITORING AGENCY REPORT NUMBER

11. SUPPLEMENTARY NOTES

12a. DISTRIBUTION/AVAILABILITY STATEMENT

Unrestricted

13. ABSTRACT (Maximum 200 words)

An experimental study has been performed to examine the three-dimensional characteristics of laminar, transitional and turbulent flow over an elliptic cone lifting body configuration. The experimental studies were performed at Mach numbers between 8 and 12 at Reynolds numbers, based on model length from 5×10^5 to 5×10^6. Detailed measurements of the distribution of heating and pressure were made along the leading edges and on the windward and leeward surfaces of the model with over 200 high-frequency, thin-film heat transfer gages and piezoelectric high-frequency pressure transducers. Measurements were also performed using temperature sensitive paints to further delineate the properties of the three-dimensional transitional flow. Schlieren photographs were also obtained of the transitional flow field over the models. Flowfield calibration measurements were made in the LENS facility with intrusive pitot and total heating transducers and nonintrusive electron beam, and infrared radiometer techniques. These data have been incorporated into the CUBRC/AFOSR Hypersonic Database which has been modified to run on the Windows platform.

14. SUBJECT TERMS	15. NUMBER OF PAGES
	54
	16. PRICE CODE

17. SECURITY CLASSIFICATION OF REPORT	18. SECURITY CLASSIFICATION OF THIS PAGE	19. SECURITY CLASSIFICATION OF ABSTRACT	20. LIMITATION OF ABSTRACT
Unclassified	Unclassified	Unclassified	None

CUBRC
Calspan - UB Research Center

P.O. Box 400
Buffalo, NY 14225
Tel. (716)631-6900
Fax (716)631-4166

EXPERIMENTAL STUDIES OF LAMINAR, TRANSITIONAL AND TURBULENT HYPERSONIC FLOWS OVER ELLIPTIC CONES AT ANGLES OF ATTACK

AFOSR Grant No. F49620-95-C-0292

Final Report

Prepared for:

United States Air Force
Air Force Office of Scientific Research
110 Duncan Avenue, Suite B115
Bolling AFB, DC 20332-0001

Prepared by:

Michael S. Holden
Calspan-University at Buffalo Research Center
Buffalo, NY 14225
(716) 631-6853

Table of Contents

SUMMARY

An experimental study has been performed to examine the three-dimensional characteristics of laminar, transitional and turbulent flow over a elliptic cone lifting body configuration. The experimental studies were performed in the Calspan 48-inch shock tunnel and the LENS facility at Mach numbers between 8 and 12 and Reynolds numbers based on model length from 5×10^5 to 5×10^6. The model employed in these studies was a 4:1 elliptical cone configuration equipped with both sharp and blunted nosetip configurations. Detailed measurements of the distribution of heating and pressure were made along the leading edges and on the windward and leeward surfaces of the model with high frequency thin-film heat transfer gages and piezoelectric high-frequency pressure transducers. The model was densely instrumented with over 200 transducers, and measurements were also performed using temperature sensitive paints to further delineate the properties of the three-dimensional transitional flow. Flowfield measurements were obtained with a highly sensitive schlieren system to provide information on the character of the transitional flow field along the axis of the body. In preparation for studies in high enthalpy flows (10,000 and 15,000 ft/sec) flowfield calibration measurements were made in the LENS facility with intrusive pitot and total heating transducers and nonintrusive electron beam, and infrared radiometer techniques. These measurements obtained in these studies provide a unique database on the mean and fluctuating characteristics of the three-dimensional transition front of a lifting body at angle of attack in high Mach number flows. These data are of key importance to the validation of models of transitional flow used in the codes to describe the shape of the transition front and length and characteristics of the transition region on air-breathing hypersonic vehicles, such as those associated with the Hy-Tech and Hyper-X programs. These data have been incorporated into the CUBRC/AFOSR Hypersonic Database which has been modified to run on the Windows platform.

1 Introduction

One of the most difficult tasks in the design of hypersonic vehicles is to predict the position and characteristics of the three-dimensional transition region on lifting bodies at angles of attack. This information is even more important for the design of air breathing vehicles where the three-dimensional characteristics of the viscous flow entering the inlet plays a key role in engine performance. In the current predictive capabilities, such as the GASP code, which are currently available for vehicle design, the position of the transition front is basically an input to the code and the length and characteristics of the transition region are based on models derived from low speed flows over flat plates or cones at zero angle of attack. Measurements on flat plates and cones in supersonic and hypersonic flow have shown the transition region is highly unsteady, yet there are no models of transition to address this flow characteristic and there is a dearth of measurements which formulate and evaluate models of transitional flow. On a three-dimensional configuration such as elliptic cone at angle of attack flow, instabilities which lead to transition come from a number of sources. In addition, the usual first and second mode instabilities observed on simple cones at zero incidence transition on delta wing/elliptic cone configurations at incidences and are influenced by instabilities introduced by crossflow (Ref. 1) and leading edge contamination (Ref. 2). How these instability mechanisms interact to control the beginning of transition on three-dimensional lifting bodies is only now being explored. However, there is almost no understanding of the mechanism which controls three-dimensional region of transitional flow, and in hypersonic flows, these regions will often cover on the order of one-third the vehicle length and therefore are of key importance. The problem of modeling these flows has generally taken second place to model transition; however, this situation must be addressed if we are to develop credible and accurate design procedure for vehicles other than the rocket propelled slender cones and blunt bodies.

This program of experimental research and analysis was conducted to begin to assemble measurements which can be used to investigate the fundamental phenomena associated with laminar, transitional, and turbulent flow over lifting body configurations designed to operate at hypersonic flow conditions. An elliptic cone configuration was selected as a generic lifting body and the experimental program has been conducted to evaluate the characteristics of flow about this body for flow regimes where laminar, transitional and turbulent flows were generated over the model. In the experimental studies, which were conducted in the Calspan 48" tunnel and the LENS hypervelocity shock tunnel, detailed flowfield and surface heat transfer and pressure measurements were made with electron beam and high-frequency heat

transfer and pressure instrumentation. Flowfield calibration studies were made to examine the freestream properties in the LENS facility employing high speed schlieren as well as pitot pressure, total temperature probes, and the electron beam. Calculations were made to predict the properties of the freestream and provide information with which to select the model configuration and the position of the instrumentation on the elliptic cone. An extensive series of studies were conducted to examine the characteristics of three-dimensional transitional flows over the leading edge and windward and leeside surfaces of an elliptic cone at angles of attack from 0 to 5 degrees. The high frequency instrumentation employed in these studies allowed us to examine both the mean and fluctuating characteristics of the transitional flows over the model. Correlations of the position of the transition front and the length and characteristics of the transition region were obtained. This information together with schlieren photographs of the flow are being included in the CUBRC/AFOSR hypersonic database which was upgraded during this study. This database contains measurements obtained in an extensive series of experimental studies of compact interacting hypersonic flows which were conducted over the past 35 years, many of which were supported by AFOSR. Recently we have modified the operating system for the database so that it can be run in Microsoft Windows or NT on an IBM compatible PC. The Windows-based system is far more user-friendly and now contains significantly more studies than the DOS version which was previously prepared and presented to AFOSR. A summary of the operation of the database is included in Section 4.

2 Experimental Program

2.1 Program Objectives and Design

The principal objective of this experimental program was to obtain detailed flowfield and surface measurements over elliptic cone lifting bodies to define the laminar, transitional and turbulent structure of the flowfields over the windward and leeward sides of the vehicle. The experimental program was conducted over a large range of Reynolds numbers at Mach numbers of 8 and 11 to investigate the flow structure from laminar to turbulent flow conditions. Flowfield measurements were conducted at velocities from 8,000 ft/sec to 15,000 ft/sec in the LENS facility to evaluate the important real-gas effects on flowfield properties. The influence of boundary layer transition on the viscous flow structure and the distribution of surface properties on the windward and leeward side of the lifting elliptic cone body configuration was the subject of major investigation in this program. Detailed measurement of the heat transfer and pressure distribution over the model provided a database with which to evaluate the models and prediction techniques to described the three-dimensional transition characteristics of the windward and leeside flows on slender lifting bodies.

The elliptic configuration selected for these studies was based on the examination of the models and measurements from earlier or current experimental studies, and computation employing state-of-the-art Navier-Stokes and DSMC codes. Examining the results from both the experimental and theoretical investigations, we examined both the models used in the numerical schemes, and the model configurations, test conditions, and instrumentation used in the experimental studies. As in all our earlier programs, the detailed design of the experimental program relied on an experimental database drawn from our experience and that generated in our other ground test programs.

2.2 Experimental Facilities

The experimental studies were conducted in Calspan's 48-inch and the LENS shock tunnel at Mach numbers ranging from 6.8 to 13, thereby spanning the regime $10^5 < Re < 6 \times 10^6$ which we believe from earlier studies is where the pressure rise occurs. The performance map for the 48-inch shock tunnel is shown in Figure 1. The operation of these tunnels can be shown simply with the aid of the wave diagram shown in Figure 2a. The tunnel is started by rupturing a double diaphragm, which permits the high-

pressure air in the driver section to expand into the driven section, and in so doing, generates a normal shock which propagates through the low pressure air. A region of high temperature, high pressure air is produced between this normal shock front and the gas interface between the driver and driven gas, often referred to as the contact surface. When the primary or incident shock strikes the end of the driven section, it is reflected, leaving a region of almost stationary high pressure heated air. This air is then expanded through a nozzle to the desired freestream conditions in the test section.

The duration of the flow in the test section is controlled by the interactions among the reflected shock, the interface, and the leading expansion wave generated by the non-stationary expansion process occurring in the driven section. At Calspan, the initial conditions of the gases in the driver and driven sections are normally controlled so that the gas interface becomes transparent to the reflect shown as shown in Figure 2a; thus, there are no waves generated by the interface-reflected shock interaction. This is known as operating under "tailored-interface" conditions. Under this condition, the test time is controlled by the time taken for the driver/driven interface to reach the throat, or the leading expansion wave to deplete the reservoir of pressure behind the reflected shock; the flow duration is said to be either driver gas limited or expansion limited, respectively. Figure 2b shows the flow duration in the test section as a function of the Mach number of the incident shock. Here it can be seen that for operation at low M_is, running times of over 25 milliseconds can be obtained with a long driver section. When run under these latter conditions at high pressures and Reynolds numbers, the test running times are of the same magnitude or longer than for piston driven tunnels (Refs. 3, 4) with comparable stagnation temperatures, and the reservoir conditions and flow quality are superior to piston driven tunnels. This results from the fact that test gas has been processed by a simple reflected shock rather than multiple shocks as in piston tunnels. A further consequence is that the freestream conditions can be calculated with far more accuracy in a shock tunnel.

LENS is a chambered shock tunnel having a 24-ft-long driver tube with an internal diameter of 12 inches and a driven tube 8 inches in diameter, which is 60 ft long. The basic layout of the LENS facility is shown in Figure 3. To achieve velocities of up to 5 km/sec, the driver section of the tunnel (shown in Figure 3) is heated to 750°F and is fitted with a stainless steel liner for hydrogen operation. The tunnel can be operated at pressures up to 30,000 psi, and, to achieve a 2 to 3 run/per-day rate, a new high-pressure, high-flow-rate compressor was installed to provide a pumping capacity that will fill the driver in approximately one hour. The driver and heater section of the tunnel are mounted on carriages that recoil with the tunnel as it is fired. A double diaphragm rig is used to accurately control the test conditions. In

this device, two diaphragms are separated by an intermediate chamber, which is held at approximately half the driver pressure; the pressure in the intermediate chamber is rapidly increased to fire the tunnel. Diaphragms over 18 inches in diameter and 1.25 inches thick are employed that are machine-scored to obtain controlled bursts with a minimum amount of fragmentation, which required a significant development program. To enable accurate studies of flowfield chemistry, cleanliness is of prime importance in the design and operation of the facility. All components that come into contact with the test gas are constructed from stainless steel, or as in the reservoir region, are constructed from copper or copper alloys. To eliminate gaps between driven-tube components resulting from the 2- to 4-million-pound recoil loads, each of the stainless steel tubes is fastened together with high-strength tensile bolts, which are pre-stressed to prevent tube separation. A centerbody apparatus, which employs a fast-acting plug valve to close the nozzle throat, is used to terminate the flow once the uncontaminated volume of shock-heated air has been exhausted from the reservoir region of the shock tube. The reservoir and centerbody region of the shock tunnel are lined with copper in order to prevent burning. Copper, molybdenum, or tungsten is used for the throat section of the tunnel to prevent melting and burning. The centerbody is a key feature for a facility designed to test fragile and expensive aero-optic components, because it prevents particulates from the diaphragm from impinging on the seekerhead window. Because the high heating rates generated in the nozzle are concentrated in a relatively small region close to the throat, the major portion of the contoured nozzle can be constructed from fiberglass. To handle the large loads generated by the recoil of the tunnel, a metal corset, which surrounds the fiberglass nozzle, is used to couple the driven tube with the test section. Shown in Figure 4 is the Mach 11 to 18 contoured fiberglass nozzle, which has an exit-plane diameter of 48 inches. Mach 8 is also available. The test section, shown in Figure 4, has an internal diameter of 96 inches and has been constructed so that it can be coupled with nozzles with exit planes up to 72 inches in diameter.

2.3 Models and Instrumentation

An elliptic cone configuration was selected for this study as typical of a hypersonic lifting body configuration after an extensive review on the database of measurements on such a configuration in non-continuum and continuum flows. The specific elliptic cone configuration was chosen to be compatible with the configurations which have been or are being employed in different but complementary studies in several other laboratories. A drawing of the elliptic cone model illustrating its shape and dimensions is given in Figure 5a. Two nosetip configurations have been constructed for this model: the sharp configuration which results in a model whose total length is 21 inches and a blunted configuration resulting in a model length

of 19-3/4 inches. The model is shown installed on the low-load sector in the 48" shock tunnel equipped with the D-nozzle in Figure 5b. In the contoured D-nozzle, measurements will be made in continuum and non-continuum flows over a range from 11 to 18. Later we will obtain measurements in the Mach number range from 6 to 8 in the contoured A-nozzle.

The elliptic cone model is highly instrumented with 212 high-frequency, thin-film and piezoelectric pressure transducers. The thin-film instrumentation has been positioned along and around the swept leading edges of the elliptical body as well as in the flatter surfaces on the windward and leeward sides of the model as shown in Figures 6 and 7. The position of the instrumentation was designed to provide highly spatially resolved measurements of the boundary layer transition process along and perpendicular to the leading edge of the vehicle in order to describe the detailed characteristics of flows associated with attachment line and cross-flow transition. The instrumentation placed on the flatter surfaces was designed to provide a detailed mapping of the transition front associated with cross-flow transition and also the characteristics of the separated region on the leeside of the elliptic cone held at angle of attack. A photograph of the model is shown in Figure 8. A major objective of the current studies is to define the large-scale, high-frequency movement of the transition front on the face of the model as well as the characteristics of turbulence through the transition process. In almost all of the earlier studies, the instrumentation that was employed did not provide information on the unsteady nature of the process or the fluctuations in the heat-transfer rate along the transition region. We also wish to provide measurements to further define the unsteady movement of two- and three-dimensional disturbances which proceed the transition process similar to that obtained on conical bodies in our earlier studies (see Ref. 5).

2.3.1 Surface Instrumentation

Heat Transfer Instrumentation – The miniature heat transfer instrumentation that was used is based on the thin-film heat transfer technique, in which a thin-film platinum resistance thermometer on a Pyrex substrate is used to sense the surface temperature of a low-conductivity surface. The transient response of this instrumentation is such that it is ideally suited to the detection of turbulent bursts and the unsteady nature of the transition region. As the heat capacity of the thin film is negligible, the film temperature is a measure of the instantaneous surface temperature of the Pyrex and is related to the heat transfer rate by the classical equation of heat transfer into a semi-infinite slab of known thermal characteristics. Analysis has shown this technique to be valid for 0.1 micron thick gages during the short

duration of a shock tunnel test. Final data reduction uses the Ray-Taulbee algorithm to relate the temperature time history to the transient heat transfer rate.

Pressure Instrumentation – The pressure transducers that would be used in this program are piezoelectric types of a design developed by Calspan and manufactured by PCB Piezotronics, Inc. (Models 103A and 103M14). These sensors have high sensitivity, and linearity generally better than 2 percent, over an operating range of about four orders of magnitude. If the linearity is not within 2 percent, a log-log curve fit is made to the calibration data, and this results in all data being within 2 percent of the curve. The Model 103A transducers have a maximum pressure capability of 3 psi. The Model 103M14 transducers have a maximum capability of 100 psi. The transducers are internally compensated for acceleration to nominal level of 0.001 psi/g.

2.3.2 Flowfield Instrumentation

Intrusive Instrumentation – Three sets of instrumentation have been used to probe the flowfield under low-enthalpy conditions. These are mean-frequency pitot probes, total-temperature probes, and thin-film probes. The Kulite-based high-frequency pitot probes have a frequency response of 30 kHz. The total temperature gages and the thin-film gages gave us the ability to measure fluctuations of up to 1 kHz and 500 kHz, respectively. Both the pitot-pressure and thin-film instruments could be used to obtain turbulent scale size in the mixing region of the flowfield.

Non-intrusive Instrumentation – Electron Beam Technique. Measurements were made using an electron-beam apparatus developed for a complementary research program (Ref. 6 and 7). Figure 9 shows the basic model configuration with the electron beam optics installed and surveying the freestream flow. The density and temperature measurement instrumentation is based on the observed relationship between the fluorescent intensity of the band system and the molecular number density. This relationship is obtained by calibration, using the same optical arrangement, over a comparable range of gas number densities and temperatures. Rotational and vibrational temperatures were determined by measuring the relative intensities of the rotational lines and vibrational bands of the emitted light. To do the former with any degree of precision, a high-dispersion spectrograph was used, which replaced the filter and photomultiplier. Vibrational temperatures are measured by splitting the light from the observed part of the beam between two or more photomultipliers, each with appropriate narrowband filters that select different vibrational bands in the spectrum.

3 Results and Discussion

3.1 Studies of Laminar, Transitional and Turbulent Flows Over an Elliptic Cone Lifting Body

3.1.1 Introduction

This phase of the experimental study was directed toward investigating the aerothermal characteristics of the transitional flow over a 4:1 elliptical cone model at angles of attack, for freestream conditions to obtain laminar, transitional and turbulent boundary layers over the cone surface. The basic objective of the investigation was to provide information with which to model the shape of the transition front and the length and properties of the transitional flow over three-dimensional lifting bodies at angles of attack. The large uncertainties in the prediction of these regions on vehicles such as those being considered for the Air Force Hy-Tech program and the NASA Hyper-X program make it of key importance to validate the theoretical prediction methods with measurements of the type obtained in this program. The experimental program was conducted in the Calspan 48" shock tunnel at Mach numbers between 8 and 12 at angles of attack from 0 degrees to 5 degrees. A key aspect to this program was the utilization of closely spaced thin-film instrumentation with the capacity to follow the turbulent fluctuations associated with the transition of the boundary layer along the leading edge and in regions of cross flow around the leading edge. High velocities that occur in hypersonic flows result in the requirement to follow frequencies above 10 kHz to accurately define the transient characteristics of the boundary layer as it transitions from laminar to turbulent flow. The thin film heat transfer instrumentation employed in this study is capable of following frequencies well above this requirement. We have also employed high-frequency pressure instrumentation capable of resolving fluctuations up to 30 kHz.

3.1.2 Discussion of Surface and Flowfield Measurements

In this experimental program, measurements were made with the elliptic cone configured with both sharp and blunted nosetips for a series of Reynolds numbers at Mach numbers of 8 and 11 to examine the effects of these parameters on the position of transition and the characteristics of the transition region. Each of these studies were repeated for angles of attack of 2.5 and 5° where measurements were made both on the windward and leeside surfaces of the model. The instrumentation package employed in this investigation is shown in Figures 7, 10 and 11 where we show the location of instrumentation on the leading edge and elliptic surface of the model. The instrumentation was situated along conical rays originating from the leading edge and the data which is plotted in the following graphs is from the six rays illustrated in Figure 11.

In the following paragraph, we briefly review some of the basic results from the experimental studies. A detailed analysis and correlation of these measurements will be published at an upcoming conference on transition. In Figures 12a and 12b, we show the variation in the distribution of heating rate to the elliptic cone surface with Reynolds number. While it can be seen that while at the lowest Reynolds number, transition on the centerline begins to occur at 8 inches back from the nosetip, increasing the Reynolds number results in the forward movement of the transition front with the centerline becoming fully turbulent along the instrumented length of the elliptic cone. Further measurements at a slightly higher Reynolds number, lower Mach number condition are shown in Figures 13a and 13b. Here we were able to obtain a fully turbulent boundary layer over almost all of the instrumented surface at the highest Reynolds number condition with transition occurring very close to the leading edge of the cone.

Placing the model at an angle of attack of 2.5 degrees, the heat transfer measurements obtained on the windward and leeside surfaces of the elliptic cone, shown in Figures 14a and 14b, respectively, demonstrate that angle of attack tends to delay transition on the leeside, and move the position for transition forward on the windward side of the model. This behavior is in contrast to measurements obtained at similar flow conditions over sharp cones (Ref. 5) where we observe transition to move forward on the leeside as angle of attack increases. Similar trends can be observed from the measurements obtained at higher Reynolds numbers shown in Figures 15a and 15b and at the lower Mach number, high Reynolds number condition in Figures 16a and 16b.We again observe that unlike the axisymmetric cone data, angle of attack at the highest Reynolds number transition moves forward on the windward side and rearward on the leeside as show in Figures 17a and 17b.

The measurements obtained at an angle of attack of 5 degrees are shown in Figures 18 through 21 provide information which again indicates that the transition front moves rearward with increasing angle of attack. In the case of the measurements shown in Figures 18a and 18b, we see that at 5 degrees incidence the leeside of the model remains the most fully laminar while there is turbulent flow along the axis of the windward surface and transitional flow across the remainder of the surface. Under the higher Reynolds number conditions shown in Figures 19a and 19b, we were able to obtain transition along the leeside line along the elliptic cone while again the windward plane exhibits a turbulent flow characteristics along most of the lower surface. Similar trends are observed in Figures 20 and 21.

The effect of bluntness illustrated in measurements shown in Figures 22a and 22b is to move the transition front rearward on both the windward and leeside surfaces of the model. The length of the transition region also appears to be lengthened as a result of surface bluntness.

In another series of studies, we examined the effect of yaw angle on the heat transfer rates along the leading edge of the elliptic cone. Measurements at yaw angles of 5 and 10 degrees shown in Figures 23 and 24 illustrate that in contrast to the measurements in the absence of yaw illustrated in Figure 25 transition begins to occur at approximately 18 inches from the tip of the model. The occurrence of leading edge transition at the greater sweep angle was consistent with predictions based on correlations obtained from earlier studies of leading edge transition (Ref. 2). Figures 26-29 are schlieren photographs of transitional flow over the elliptic cone.

Measurements obtained in these studies are presently being compared with laminar and turbulent flow predictions employing the GASP code and correlations of the position and transition and the characteristics of the transition region are being assembled to aid in the selection of models to be employed to calculate the streamwise variation of heat transfer rate in the transition region.

3.2 Calibration of Hypervelocity Flowfields Employing Intrusive Instrumentation and Electron Beam Techniques

3.2.1 Introduction

During this program, we have employed an electron beam apparatus to obtain density and species measurements to define the characteristics of the nonequilibrium hypersonic flows, encountered under some of our high enthalpy conditions. The electron beam apparatus has in the past been used extensively to obtain measurements in low-density flows in these studies we have employed an electron-beam gun which enables measurements to be obtained under higher pressure conditions where transitional and turbulent flows can exist. This set of measurements were designed to not only provide flowfield calibration data but also yield a set of measurements which can be used to validate the models of flowfield density employed in our nonequilibrium nozzle code. The electron beam instrumentation is capable of following the high frequency density fluctuations which occur in the boundary layer during the transition process as demonstrated in Reference 7.

3.2.2 Flowfield Measurements

The electron beam apparatus was installed in a specially designed survey model to obtain measurements of the freestream characteristics of hypervelocity flows. The model which contained the electron beam is shown installed in the LENS facility in Figure 30. A schematic diagram of the electron beam installed in the survey model positioned to survey the flow in the LENS facility is shown in Figure 9. This apparatus was used in a series of studies to define the nonequilibrium composition of the flow at velocities of 10,000 and 15,000 ft/sec where vibrational and chemical nonequilibrium occurred. Typical measurements of the nitrogen spectrum which are employed to provide information on the vibrational and rotational temperature of the gas are shown in Figure 31. Similar data are also shown of NO radiation in Figure 32 from measurements to define the magnitude of this constituent of the flow. Measurements of the mean freestream density and temperatures made with the electron beam were found to be in good agreement with nozzle flow calculations. Figure 33 a and b shows a comparison between the time histories of pitot pressure and CO_2 radiation signal obtained at 14,200 ft/sec illustrating that both the aerodynamic and aerothermodynamic properties of the flow provide comparable useful test times of close to 6 milliseconds at this condition.

In an additional electron beam study, an extensive series of calibrations and measurements were made in an attempt to use this apparatus to determine the end of the run by detecting the occurrence of

helium or a trace gas in the flow which originated in the driver section of the tunnel. Helium is used as a driver gas for a number of high-temperature conditions; while a trace gas can be added to either the double diaphragm set and the tunnel or the driver. We wished to excite this gas by the electron beam and thereby provide definitive measurements of when the driver gas is present in the test flow. A number of additives such as argon and xenon were tested as to their effectiveness as a tracer; however, although we were able to employ the electron beam to excite these gas in a static calibration rig after an extensive series of tests, we were unsuccessful in using such an approach to positively define the end of the useful test time of the flow.

4 Assembly and Refinements of the CUBRC/AFOSR Hypersonic Database

4.1 Introduction

One of the most important outputs of an experimental program, in addition to the improved understanding of the phenomenology, is the assembly of measurements which can be used to develop and refine models of the key phenomena controlling the characteristics of the flow. With the development of DSMC and Navier-Stokes codes capable of accurately defining the characteristics of laminar flow of a perfect gas, the emphasis has now swung to understanding and modeling real gas phenomena in laminar flows and transitional and turbulent mixing phenomena for flows at Reynolds numbers larger than those required to maintain fully laminar flow. From the viewpoint of the design of hypervelocity vehicles, the most critical design areas are associated with the high aerothermal loads which occur in regions of shock wave/boundary layer and shock/shock interaction, and the efficiency of active cooling techniques which are in many cases required to alleviate the aerothermal loads in such regions. The experimental studies conducted for AFOSR during the past 35 years have been highly oriented toward the investigation of such phenomena, and from these studies, we have selected the most useful and accurate sets of measurements to be included in the CUBRC database. The measurements placed in the database fall into four basic areas: (1) measurements made in laminar flows on simple flow configurations as well as in regions of shock wave boundary layer interaction and shock/shock interaction; (2) measurements in transitional flows over simple model configurations as well as on configurations involving adverse and favorable pressure gradients and cross flows; (3) measurements made in turbulent flows over simple configurations as well as those in regions of shock/shock and shock boundary layer interaction; and (4) measurements of the performance and effectiveness of active cooling techniques such as film and transpiration cooling with and in the absence of regions of shock/shock and shock boundary layer interaction. All of the measurements provided in this database were for well-defined model and flowfield configurations with instrumentation capable of high resolved temporal and spatial resolution.

As discussed earlier, we have recently upgraded the system which controls the database so that it can be operated in a Windows 95 environment with the result that it is more easily operated by users familiar to the PC Windows environment. This recent upgrade is described in Appendix 1.

4.2 Review of CUBDAT Database Program

4.2.1 Overview

CUBDAT is a program designed to provide access to reduced data from experimental studies conducted in Calspan's shock tunnels from 1964 to the present. Available to qualified users, CUBDAT can only be run on PC's running Microsoft® Windows® 95 or NT, there are no plans to develop versions for other platforms. Interaction with CUBDAT is consistent with the standard Windows interface, although its overall design is based on the previous, DOS version (see "A Database of Aerothermal Measurements in Hypersonic Flow for CFD Validation" AIAA 92-4023).

Data for CUBDAT is stored in binary files with the extension .STY. These study files contain data from a number of runs as well as test conditions and summary information. Each study requires that a separate text file containing the abstract present in the same directory. Individual runs can be exported in a delimited text format compatible with most spreadsheet programs.

Runs are divided into sixteen groups, representing different sensor positions or conditions. While every run is divided in this manner, not all groups contain data; often only the one or two groups will contain data. Runs may also include a time index, indicating the time (in milliseconds) from the start of the run that the data represents.

4.2.2 Viewing Data

To open a study for analysis, select "Open study" from the File menu, select the file you wish to open, and click the "Open" button. To view the data or test conditions for a run, the user must first select a default run. To do this, choose "Select run î from the Data menu and choose a run from the list provided. Selecting "View test conditions" will display the test conditions for the default run. Selecting "View run data" will display all of the data associated with the default run. To copy text to the Windows Clipboard, choose "Copy to clipboard" from the Data menu.

Once a default run has been selected, it can be exported as delimited text, a generic format that can be read by most spreadsheet programs. To do this, select "Export run as text" from the "File" menu. The data will be saved with tabs separating columns and carriage returns separating rows.

4.2.3 Plotting Data

Once a study has been open, different data from various runs may be plotted for analysis. Plots are set up by selecting "Define variables" from the Plot menu. This will bring up the variable definition window. Up to sixteen different data sets (referred to here as variables) may be plotted simultaneously. The instructions that follow define a single variable, to plot multiple variables, select a different variable from the list at the top of the window and repeat the procedure.

To include a variable in the plot, check the "Variable Active" box. The "Plot Style" box controls the appearance of the variable. To change the color, double-click in the "Color" box. If "Line" is checked, lines will be drawn between data points. If "Symbol" is checked, the symbol indicated in the symbol list will be plotted at each point.

The "Run Number" list selects the run from which the variable will draw its data. The "Data Type" list selects the type of data (pressure, heat transfer rate, etc.) for the variable. The "Normalizing Factor" list selects the factor used to non-dimensionalize the data; factors can be selected from the list or a numerical value may be entered. The "Active Groups" box determines which groups (of the selected run) will be included in the variable. Use the "Activate All" and "Deactivate All" buttons to quickly enable or disable all groups. Finally, the "Name" box contains the legend entry for the variable.

Once all variables have been defined, click the "OK" button to view the plot.

To change the domain and range of the plot, select "Adjust range" from the Plot menu. "Set symbol size" allows the user to change the size of the symbols used in the plot (default is 3 pixels). "Set axis titles" allows the user to change the names of the axes. "Set plot font" allows the user to change the font used in the plot (default is Times New Roman, 14pt).

To fit a polynomial to a variable, select "Fit" from the "Polynomial fit" sub-menu. The variable to which the curve will be fitted is selected from the list at the top of the Polynomial fit window. Enter the degree of the curve in the "Degree of fit" box. The color of the fit curve is set with the "Color" box (double-click to change). If the "Draw fit" box is checked, the curve will be drawn on the plot. If the

"Legend entry" box is checked, the equation of the curve will be included in the legend. The equation of the curve can also be found by selecting "View coefficients" from the "Polynomial fit" sub-menu.

To copy a plot to the Windows clipboard, select "Copy to clipboard" from the Data menu. The plot will be copied as a scalable Windows metafile. Due to inconsistencies in the treatment of metafiles between programs, plots may not copy exactly. On some programs, sideways text may appear as horizontal on the screen, however it should appear properly when printed.

4.2.4 .STY File Format

This section is provided for those who wish to access CUBDAT data directly. Information given in this section is based on the C/C++ language.

4.2.5 Data Types

Type	Size(bytes)	Range
char	1	-128 to 127
unsigned char	1	0 to 255
short int	2	-32,768 to 32,767
int	4	-2,147,483,648 to 2,147,483,647
float	4	$-3.4 \times 10^{+38}$ to $3.4 \times 10^{+38}$

A number within braces ([]) indicates an array. For example, int Array[10] indicates an array of 10 four-byte integers, with indices from 0 to 9, inclusive.

4.2.6 Data Structures

The following data structures are the same as those used within CUBDAT to store data. Placing structures within structures may cause confusion, but it provides a convenient way to organize the data.

The _RunID structure identifies each run in a study by number and time index. A value of -1 for Time indicates that there is no time index associated with the run.

```
struct _RunID
{
 short int Number;
 float Time;
};
```

The _StudyInfo structure contains the summary, abstract filename, group labels, and a list of the run numbers that appear in the file.

```
struct _StudyInfo
{
 char Name[64];                //the name of the study
 char SummaryInfo[1024];       //summary text
 char AbstractFilename[256];   //the file name of the abstract
 char GroupLabel[16][32];      //sixteen group labels
 char AxisLabel[64];           //the default label for the x-axis
 unsigned char NumRuns;        //number of runs
 _RunID RunList[256];          //included run numbers
};
```

The _DataPoint structure holds the group number, position, and value of a single data point.

```
struct _DataPoint
{
 unsigned char GroupNumber;    //acceptable values from 0 to 15
 float Position;
 float Value;
};
```

The _DataSet structure is essentially an array of _DataPoints.

```
struct _DataSet
{
 unsigned char NumData; //number of data points
 _DataPoint Data[256];  //array of data points
};
```

The _Run structure contains test conditions and one _DataSet for each type of data (pressure, skin friction, etc.)

```
struct _Run
{
 _RunID ID;        //this run's identification

 float Po;         //reservoir total pressure
 float Ho;         //reservoir total enthalpy
 float To;         //reservoir total temperature
 float Hw;         //wall enthalpy
 float Tw;         //Wall temperature
 float Mi;         //shock tube incident mach number
 float M;          //freestream mach number
 float U;          //freestream velocity
 float T;          //freestream temperature
 float P;          //freestream static pressure
 float Rho;        //freestream density
 float Mu;         //freestream viscosity
 float Re;         //freestream Reynolds number
 float Pop;        //Pitot pressure (Po')
 float Q;          //dynamic pressure
 float CPf;        //pressure to CP factor
 float CHf;        //heat rate to CH factor
 float QoFR;       //Fay-Riddell heat transfer

 char ExtraTC[16][64];  //16   additional   test conditions (64-
                        //character strings)

 _DataSet DataSet[7]; //see below
};
```

DataSet[0] = pressure data

DataSet[1] = skin friction

DataSet[2] = force/moment

DataSet[3] = heat transfer rate

DataSet[4] = surface temperature

DataSet[5] = calorimeter

DataSet[6] = miscellaneous

4.2.7 File Format

The first item in any .STY file is a `_StudyInfo` structure. There then follows one `_Run` structure for each run listed in `_StudyInfo.RunList`. `_Run` structures appear in the same order as their entries in `_StudyInfo.RunList`

5 References

1. Holden, M.S., Bower, D.R., and Chadwick, K.M., "Measurements of Boundary Layer Transition on Cones at Angle of Attack for Mach Numbers from 11 to 13," Report No. 2610-4, Contract F33601-89-D-0045, prepared for University of Dayton Research Institute, May 1994.

2. Holden, M.S. and Kolly, J.M., "Attachment Line Transition Studies on Swept Cylindrical Leading Edges at Mach Numbers from 10 to 12," AIAA 95-2279, paper presented at the 26th AIAA Fluid Dynamics Conference in San Diego, CA, June 19-22, 1995.

3. Calspan Hypersonic Shock Tunnel, Description and Capabilities Brochure," 1975

4. Holden, M.S., "Large-Energy National Shock Tunnel (LENS) Description and Capabilities," Brochure, February 1991.

5. Holden, M.S., Bower, D.R. and Chadwick, K.M., "Measurements of Boundary Layer Transition on Cones at Angle of Attack for Mach Numbers from 11 to 13," AIAA 95-2294, paper presented at the 26th AIAA Fluid Dynamics Conference in San Diego, CA, July 10-12, 1995.

6. Holden, M.S., "Real Gas Effects on Regions of Viscous-Inviscid Interaction in Hypersonic Flows," AIAA 97-2056, paper presented at the 28th AIAA Fluid Dynamics Conference, 4th AIAA Shear Flow Control Conference, Snowmass Village, CO, June 29-July 2, 1997.

7. Holden, M.S., Harvey, J., Bergman, R.C., Boyd, I.D., DeLeon, R., "Experimental and Theoretical Studies of Real Gas Effects, Shock Interaction and Turbulent Mixing and Combustion in Hypervelocity Flows," Final Report, U.S.C. PO 630812, September 1997.

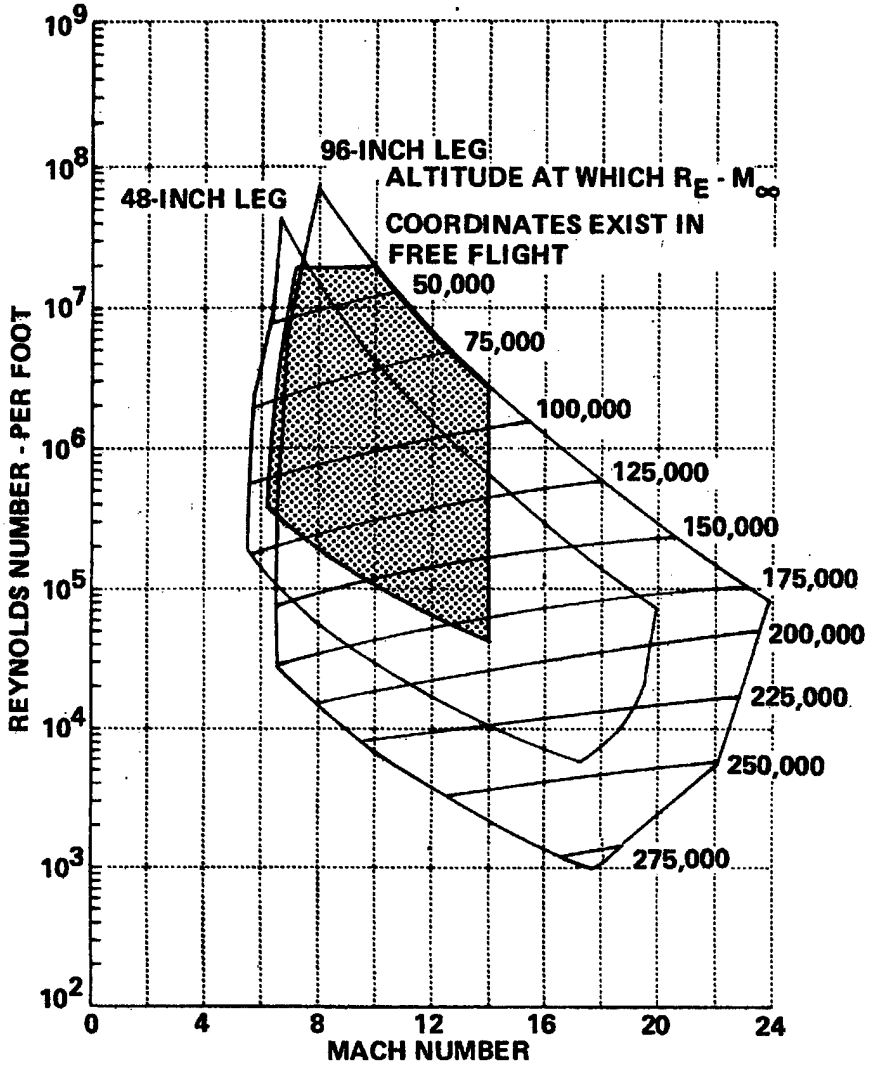

Figure 1 **PERFORMANCE MAP FOR 48-INCH AND 96-INCH SHOCK TUNNELS**

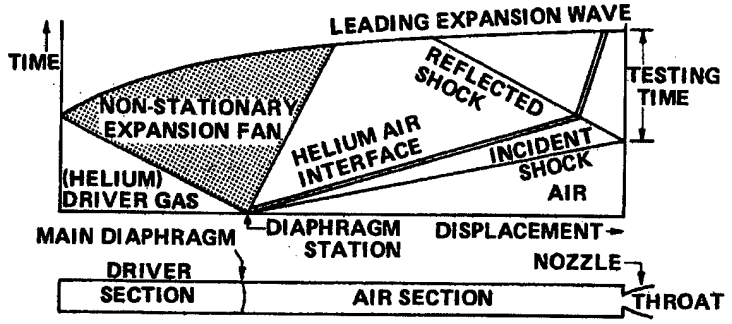

(a) WAVE DIAGRAM FOR TAILORED-INTERFACE SHOCK TUBE

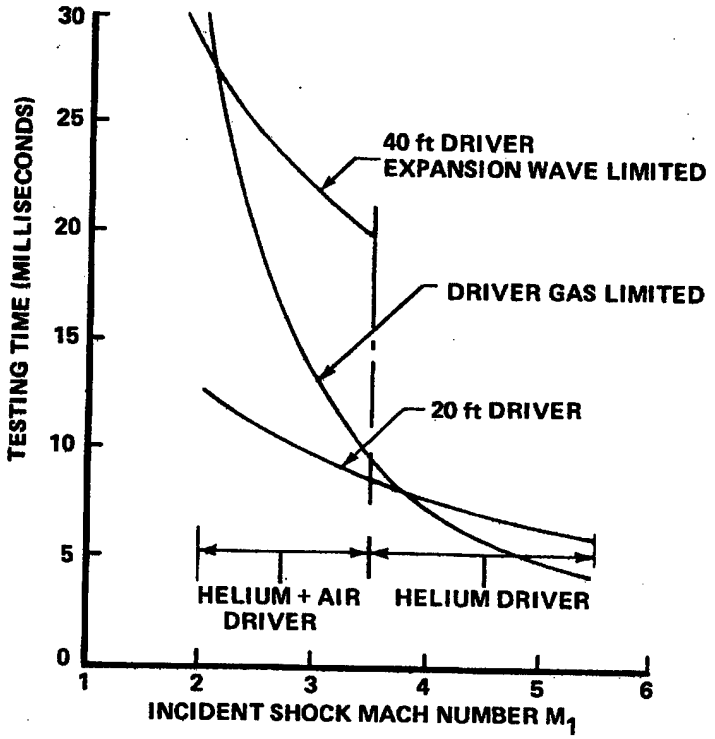

(b) TEST TIME AVAILABLE FOR TAILORED INTERFACE OPERATION OF THE SHOCK TUNNEL

Figure 2 **PERFORMANCE CHARACTERISTICS OF CALSPAN'S 48" SHOCK TUNNEL**

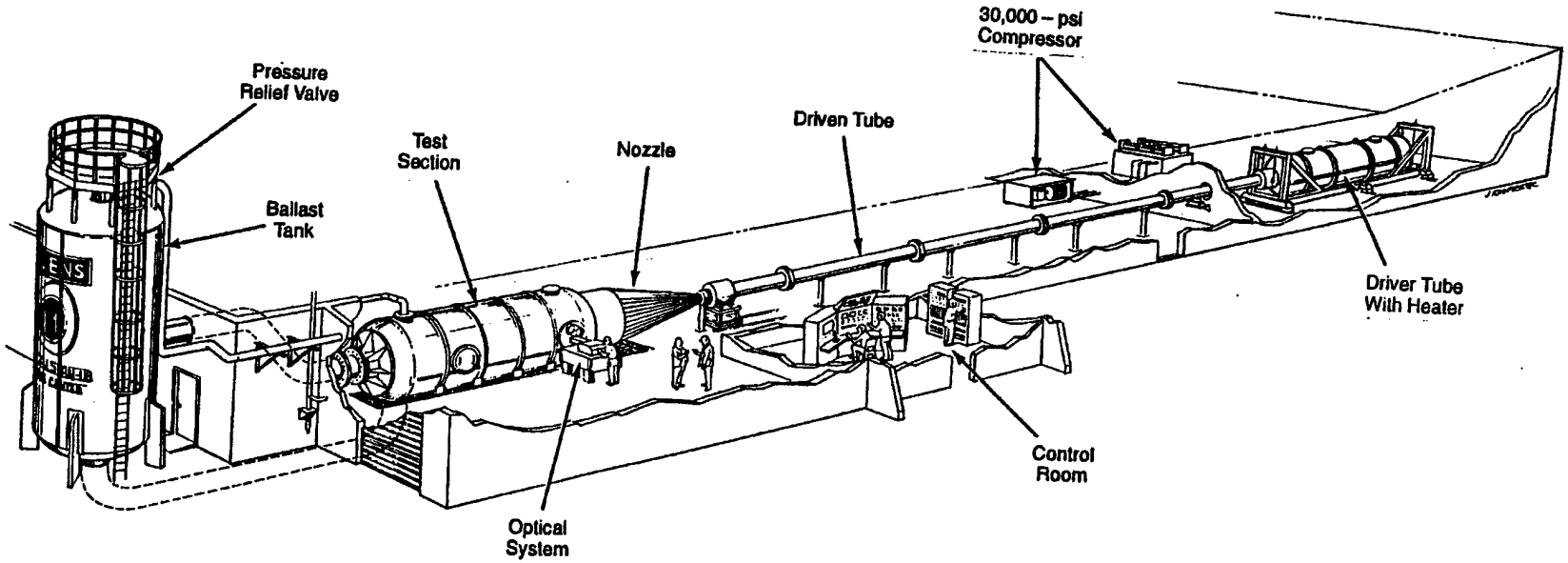

Figure 3 PHYSICAL LAYOUT OF LARGE ENERGY NATIONAL SHOCK (LENS) TUNNEL

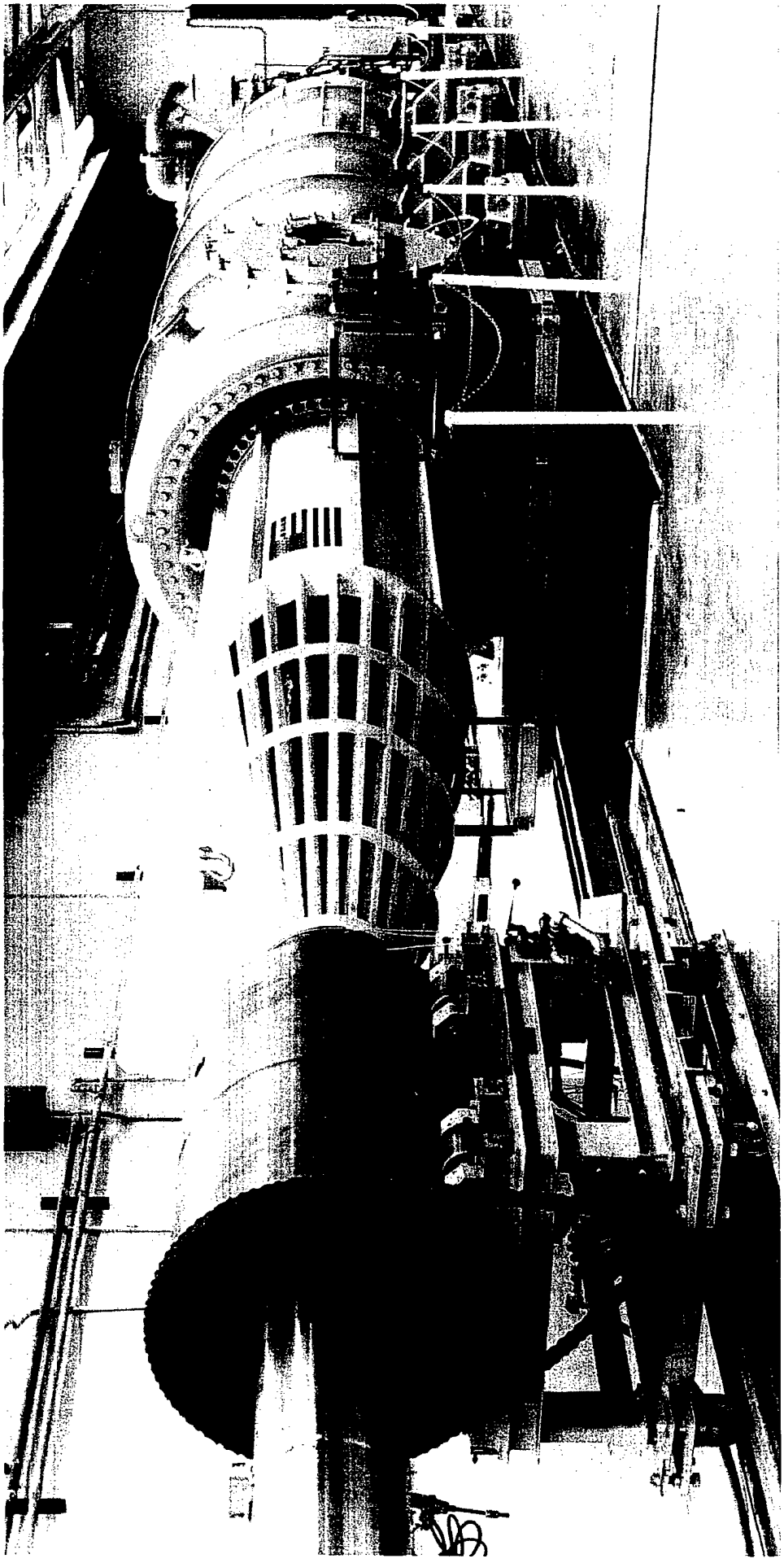

Figure 4 DRIVEN TUBE AND NOZZLE SECTION OF THE LENS FACILITY

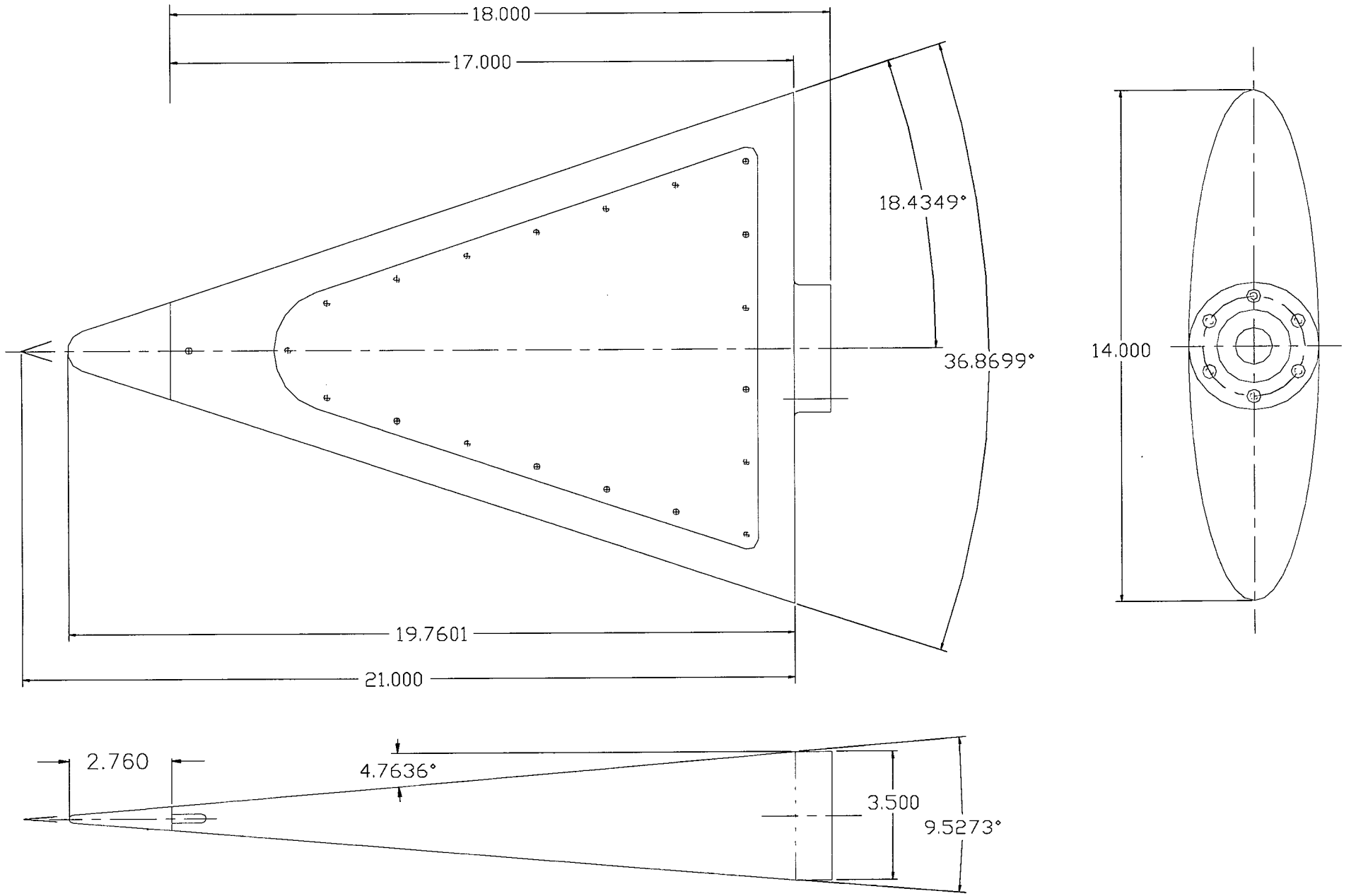

Figure 5a DRAWING OF ELLIPTICAL CONE MODEL

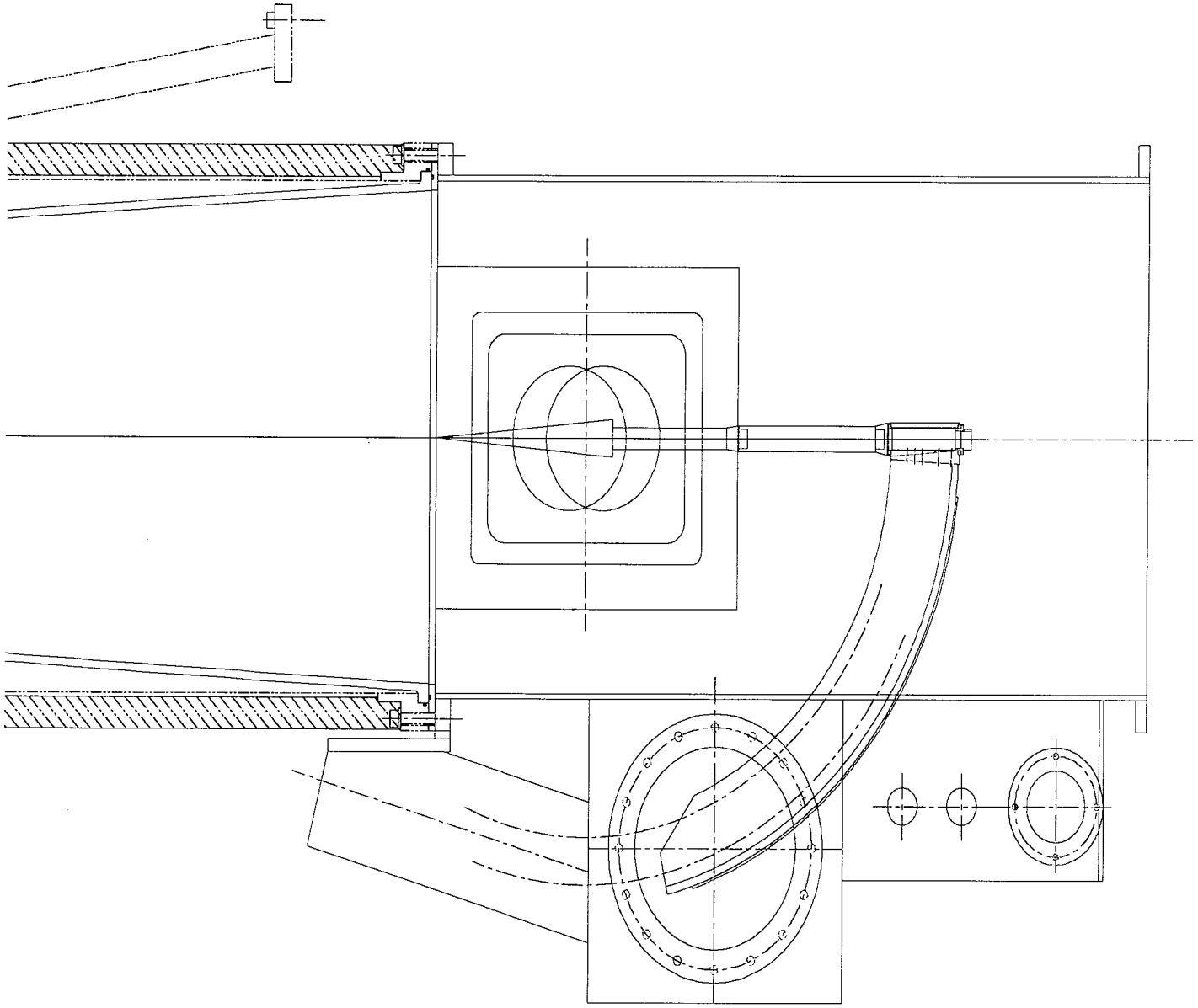

Figure 5b ELLIPTIC CONE INSTALLED IN D-NOZZLE

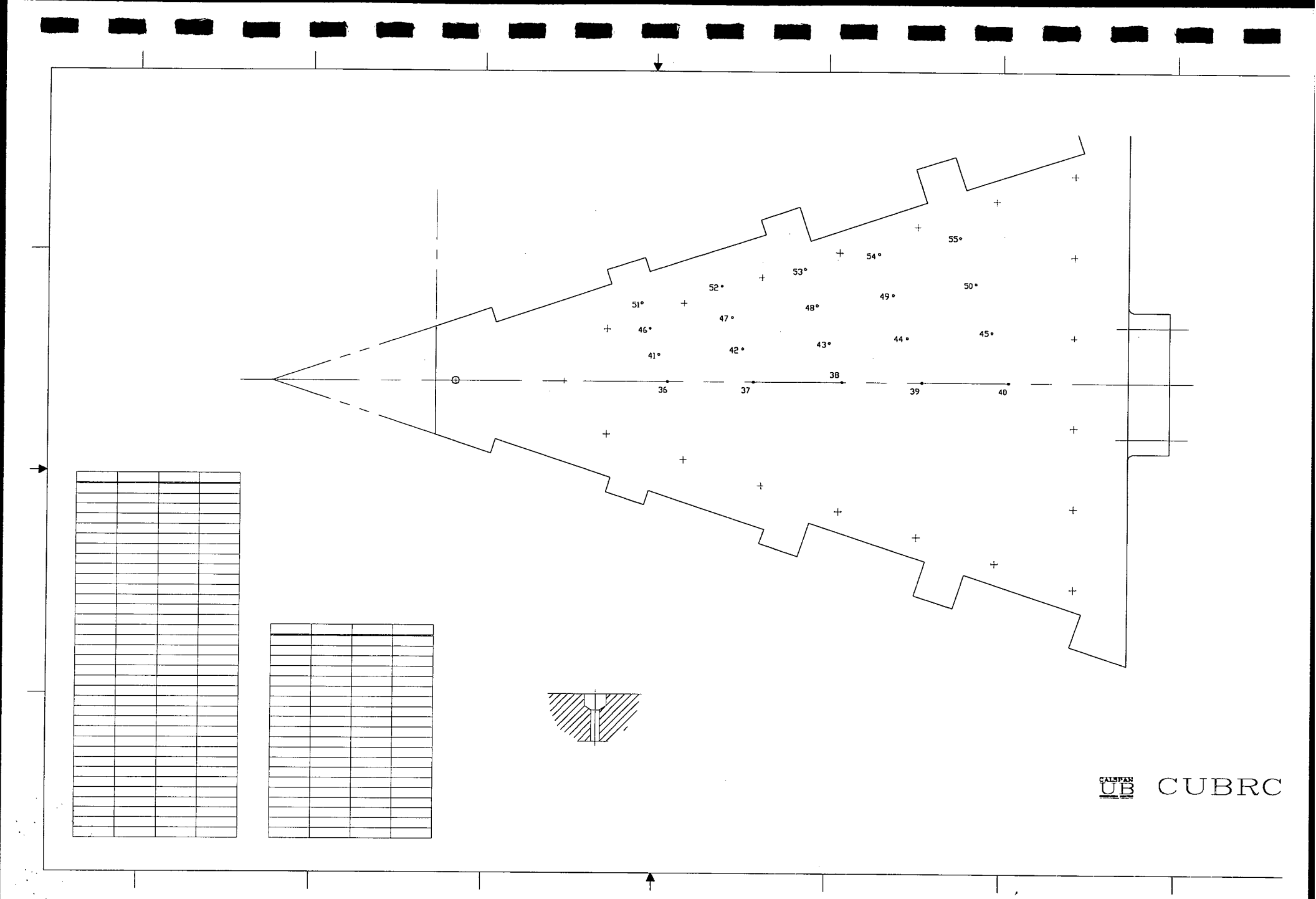

Figure 6 LOCATION OF HEAT TRANSFER AND PRESSURE INSTRUMENTATION ON FACE OF ELLIPTICAL CONE MODEL

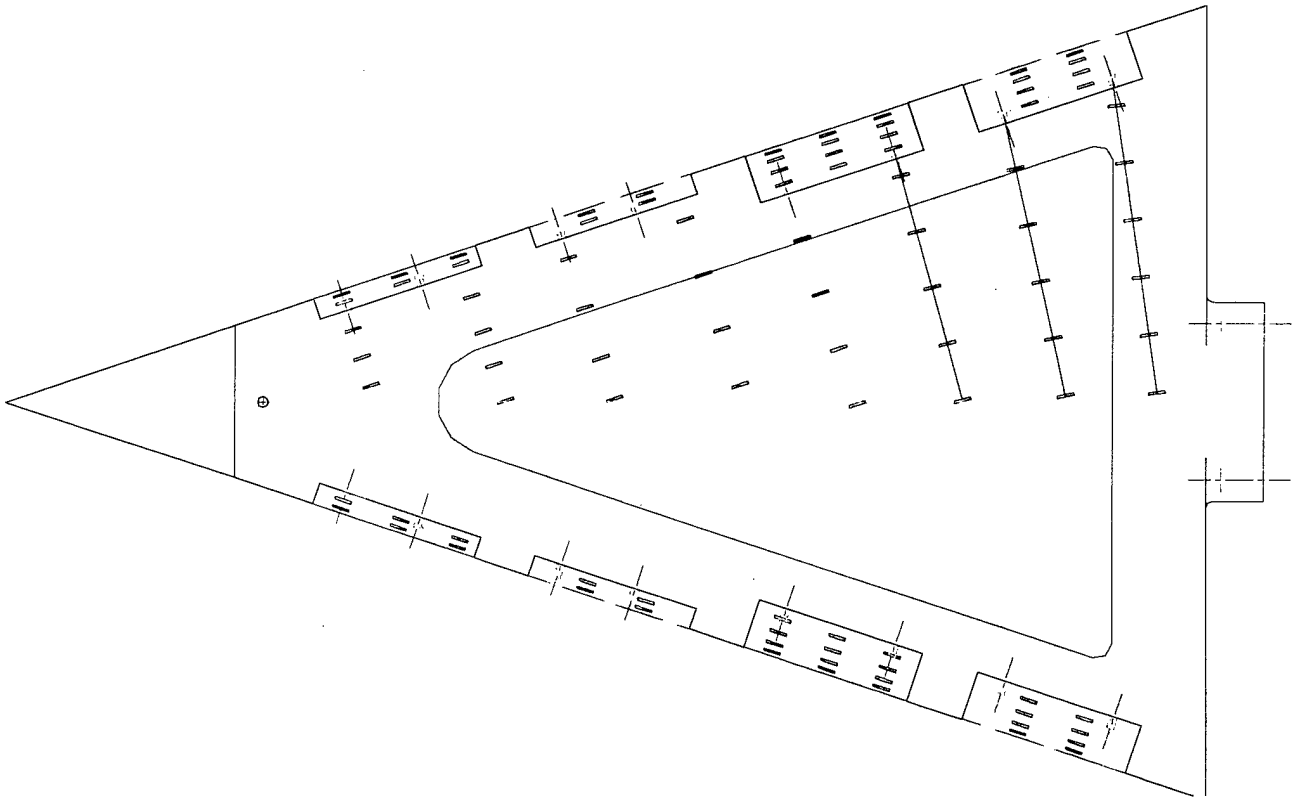

Figure 7 LOCATION OF LEADING EDGE INSTRUMENTATION ON ELLIPTICAL CONE MODEL

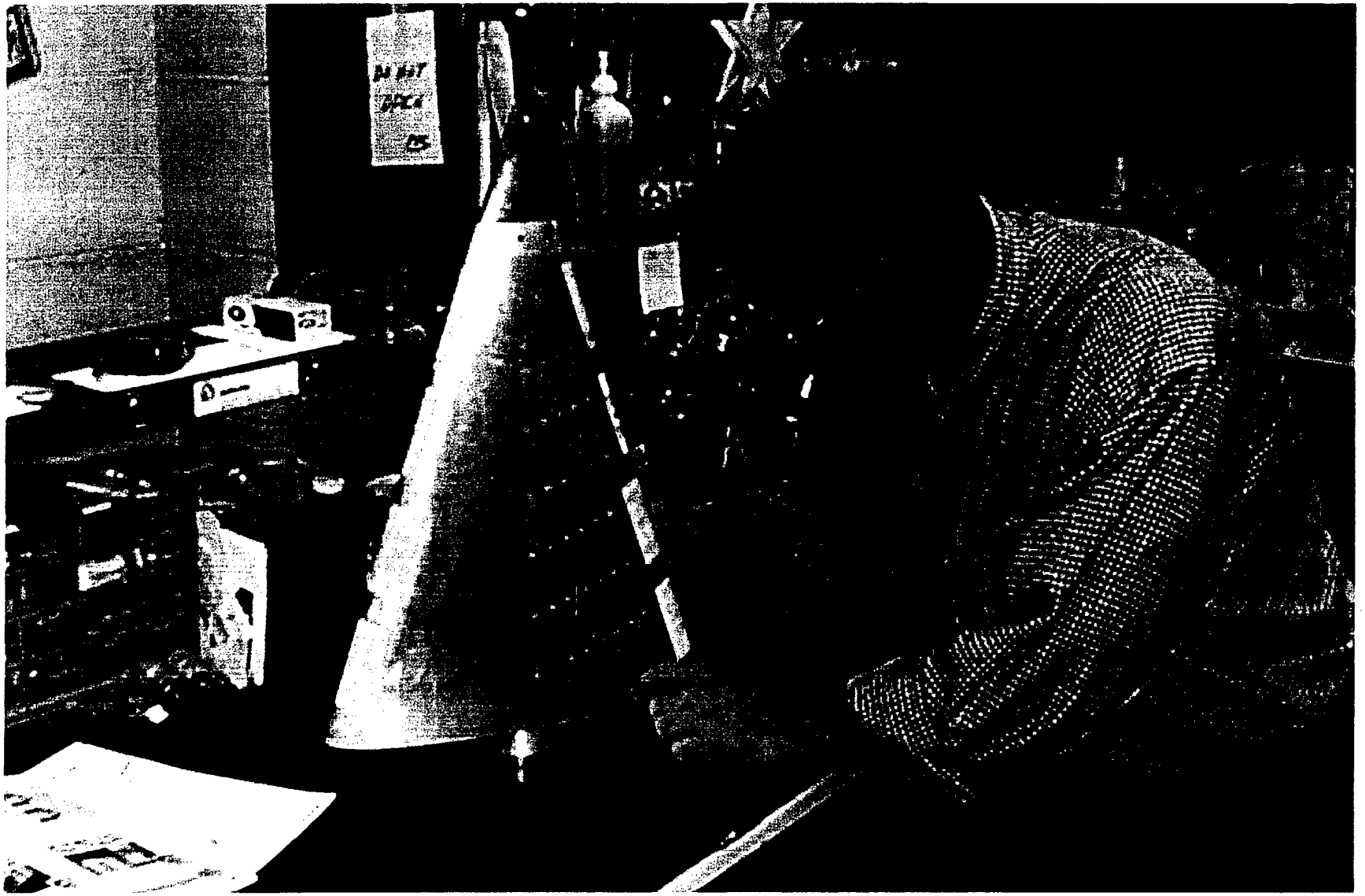

Figure 8 Thin-Film Instrumentation Along and Around Elliptical Body (Windward and Leeward Sides)

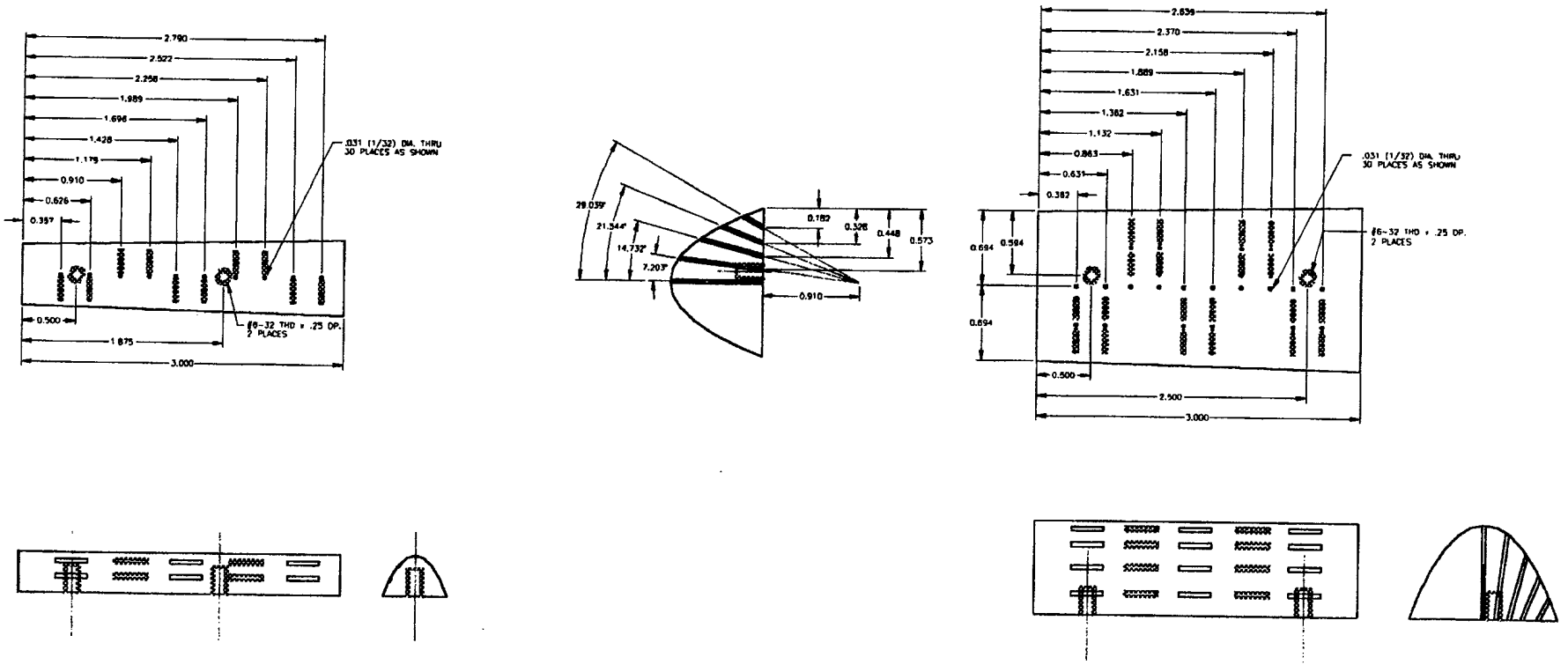

Figure 9 **LOCATION OF THIN-FILM GAGES ON LEADING EDGE SURFACES**

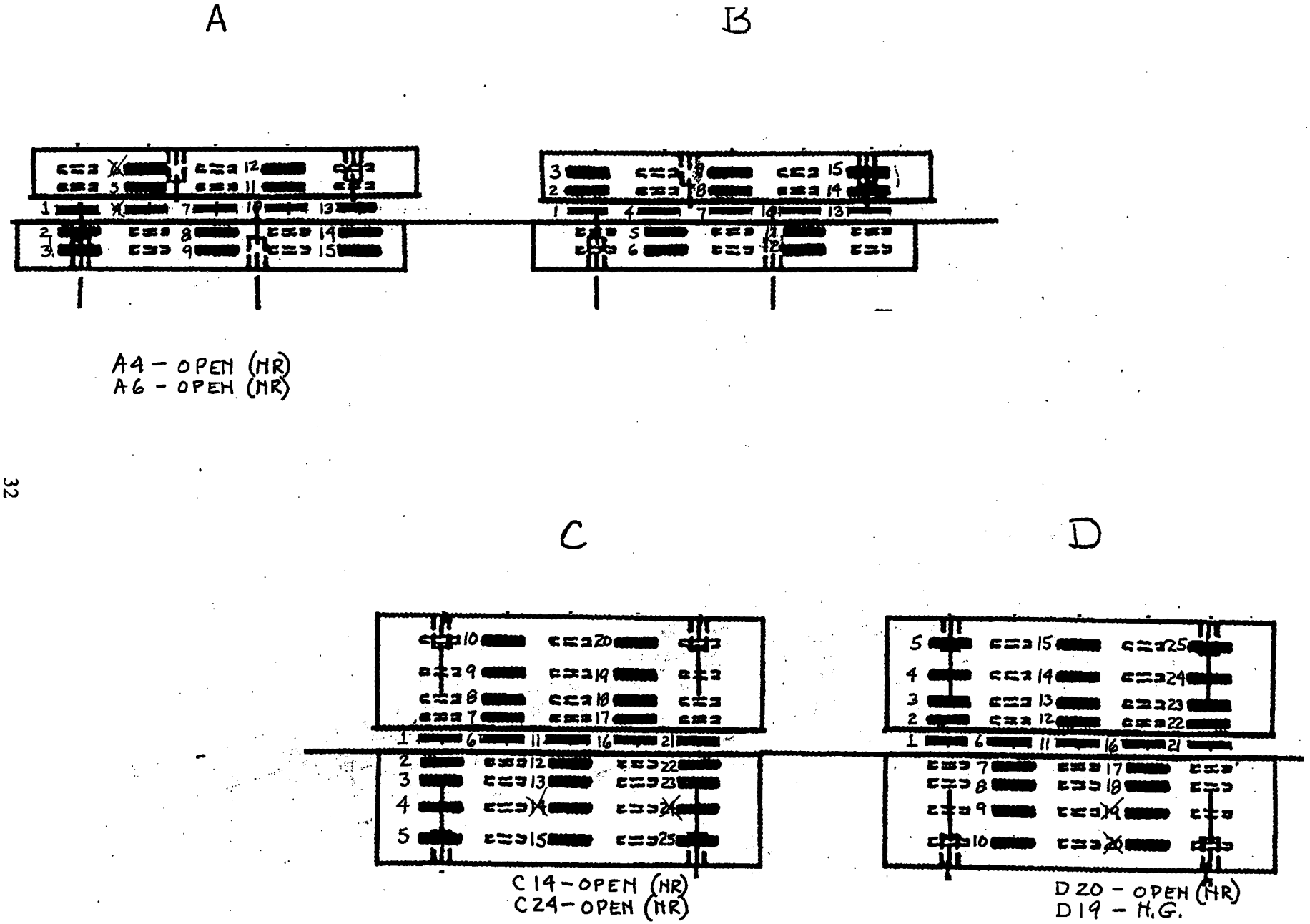

Figure 10 LOCATION OF LEADING EDGE GAGES ON ELLIPTIC CONE MODEL

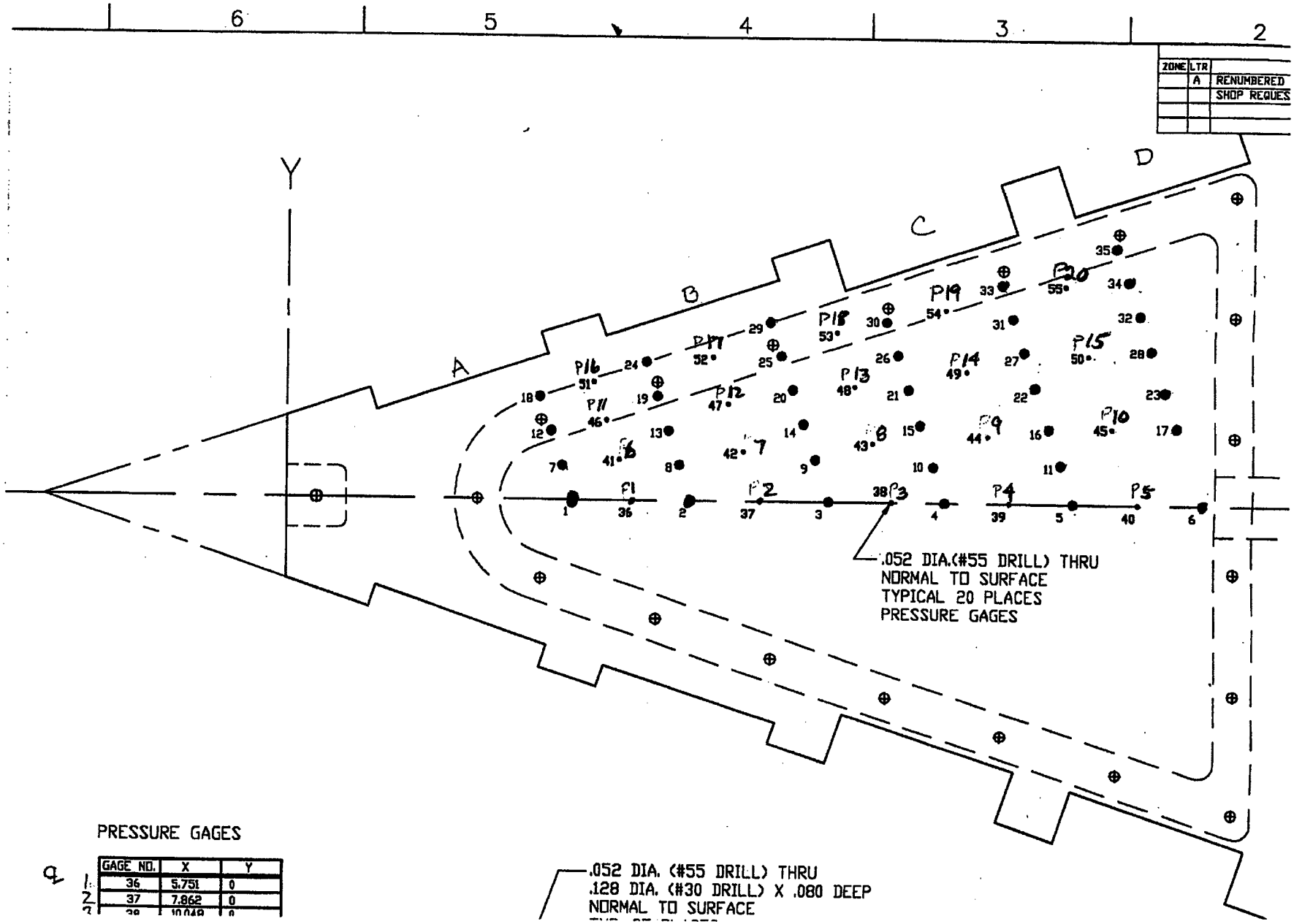

Figure 11 INSTRUMENTATION ALONG CONICAL RAYS ORIGINATING FROM LEADING EDGE

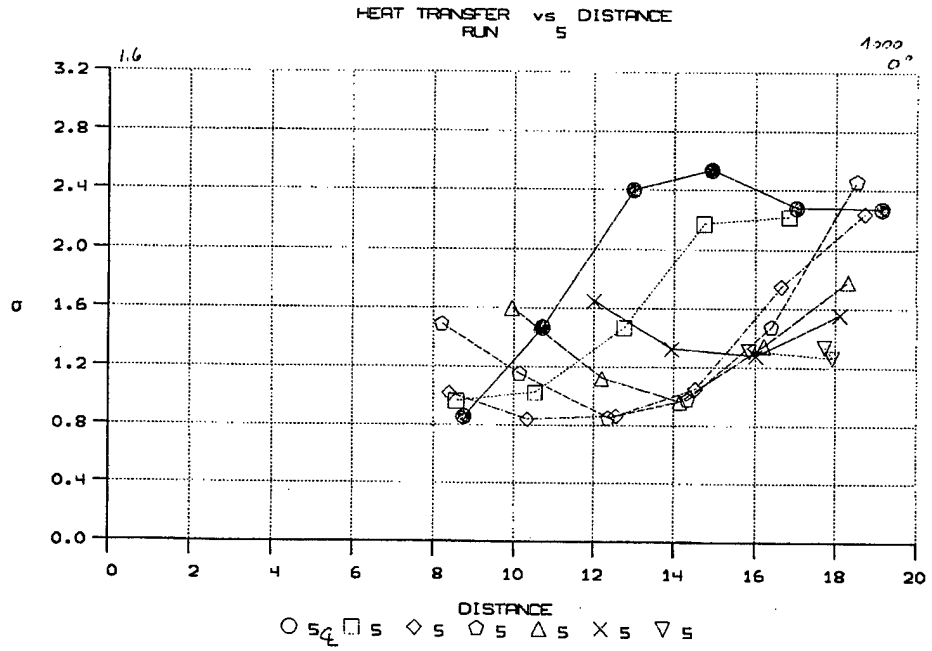

Figure 12a TYPICAL HEAT TRANSFER MEASUREMENTS IN TRANSITIONAL FLOW REGION OVER SHARP CONE AT MEDIUM REYNOLDS NUMBER FOR MACH 11 FLOW

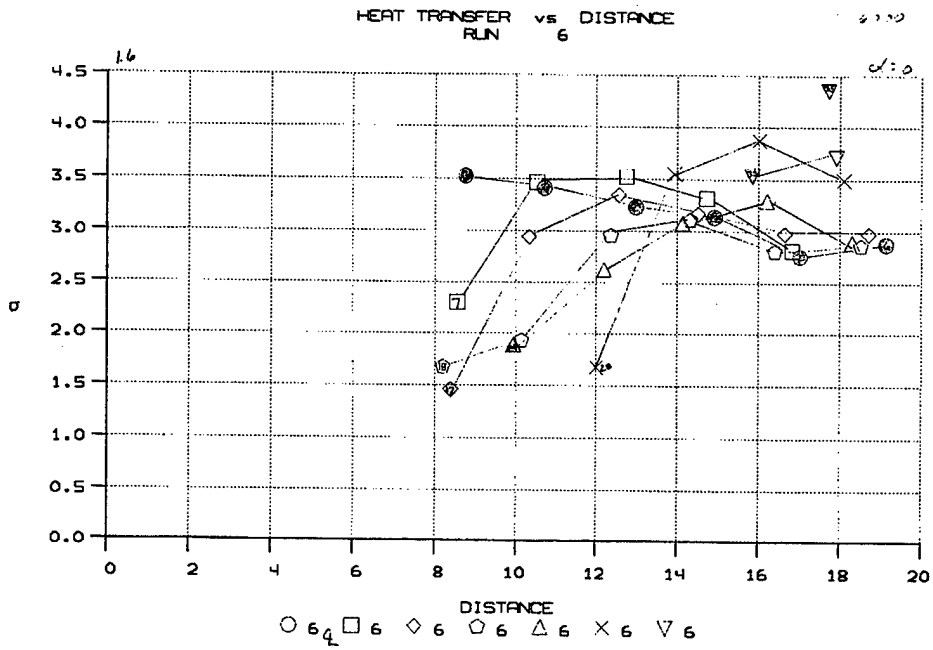

Figure 12b TYPICAL HEAT TRANSFER MEASUREMENT IN TRANSITIONAL FLOW OVER SHARP CONES AT HIGH REYNOLDS NUMBER FOR MACH 11 FLOW

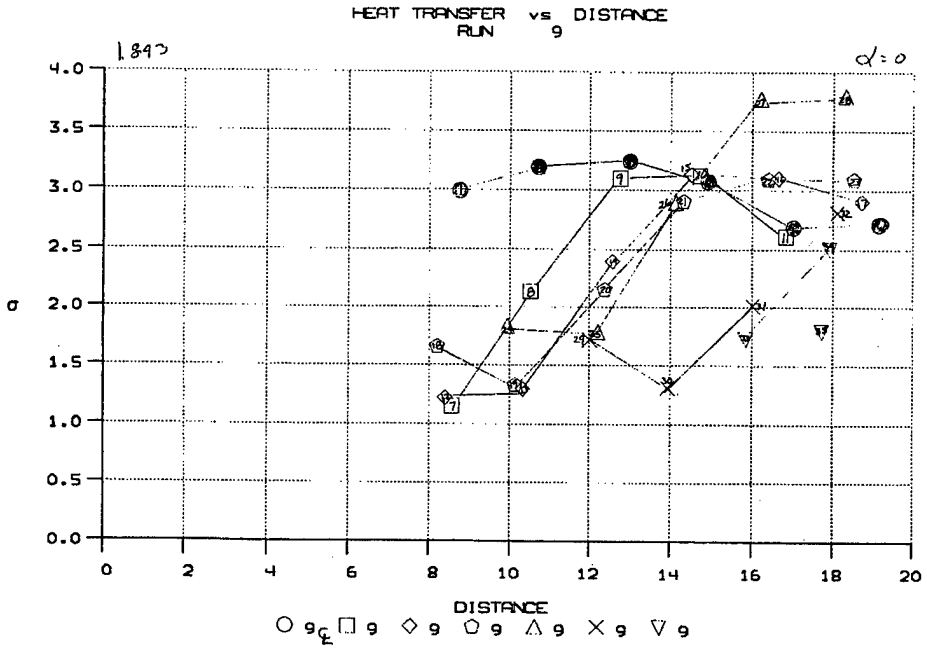

Figure 13a **TYPICAL HEAT TRANSFER MEASUREMENTS IN TRANSITIONAL FLOW OVER SHARP ELLIPTIC CONE AT MEDIUM REYNOLDS NUMBER IN MACH 8 AIR-FLOWS**

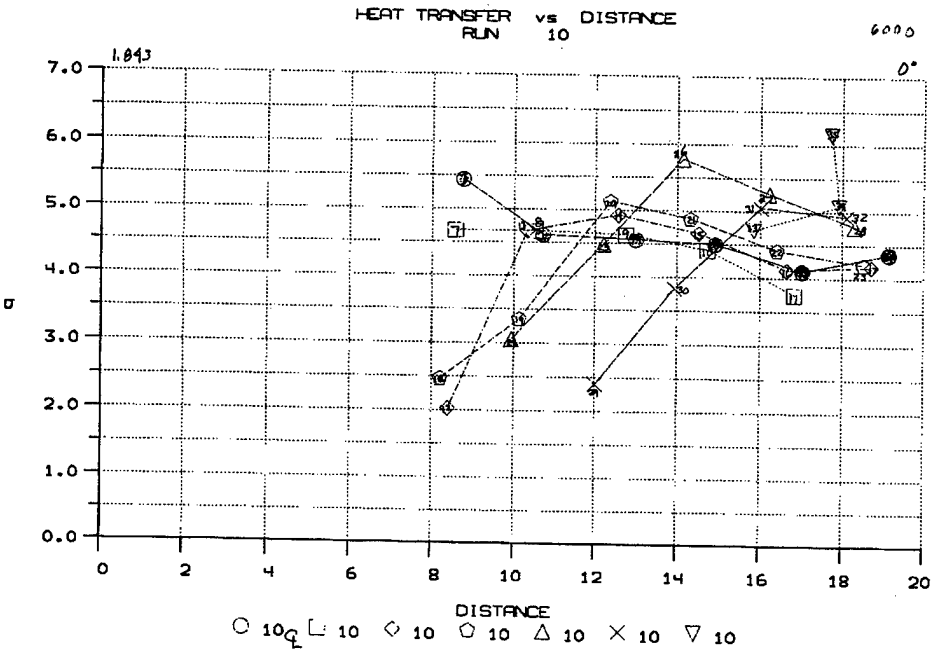

Figure 13b **TYPICAL HEAT TRANSFER MEASUREMENTS IN TRANSITIONAL FLOW OVER SHARP ELLIPTIC CONE AT HIGH REYNOLDS NUMBER IN MACH 8 AIR-FLOWS**

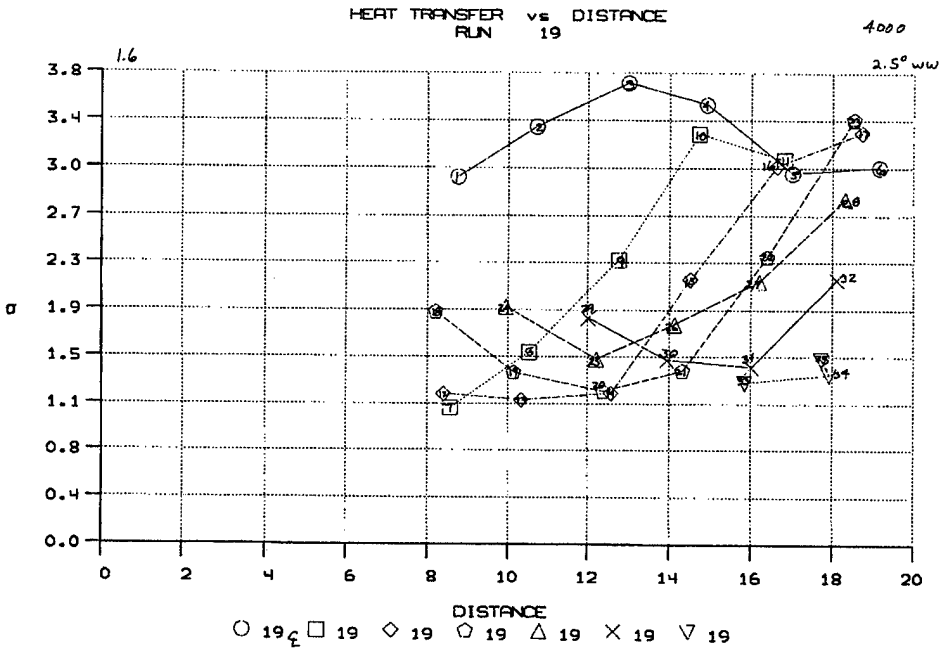

Figure 14a **TYPICAL HEAT TRANSFER MEASUREMENTS ON WINDWARD SURFACE ON SHARP ELLIPTIC CONE AT 2.5° INCIDENCE AT MEDIUM REYNOLDS NUMBER AT MACH 11**

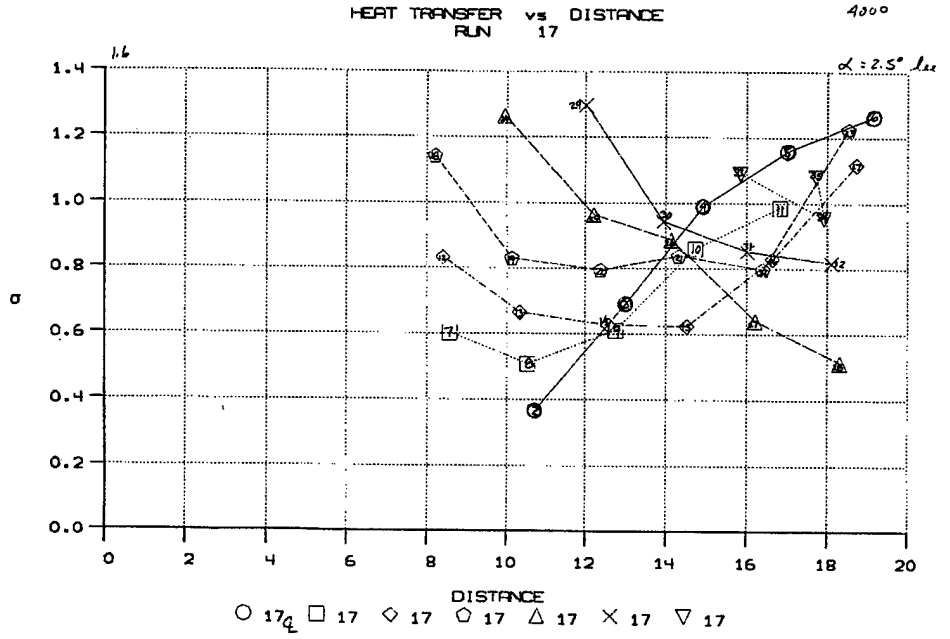

Figure 14b **TYPICAL HEAT TRANSFER MEASUREMENTS ON LEESIDE SURFACE ON SHARP ELLIPTIC CONE AT 2.5° INCIDENCE AT MEDIUM REYNOLDS NUMBER AT MACH 11**

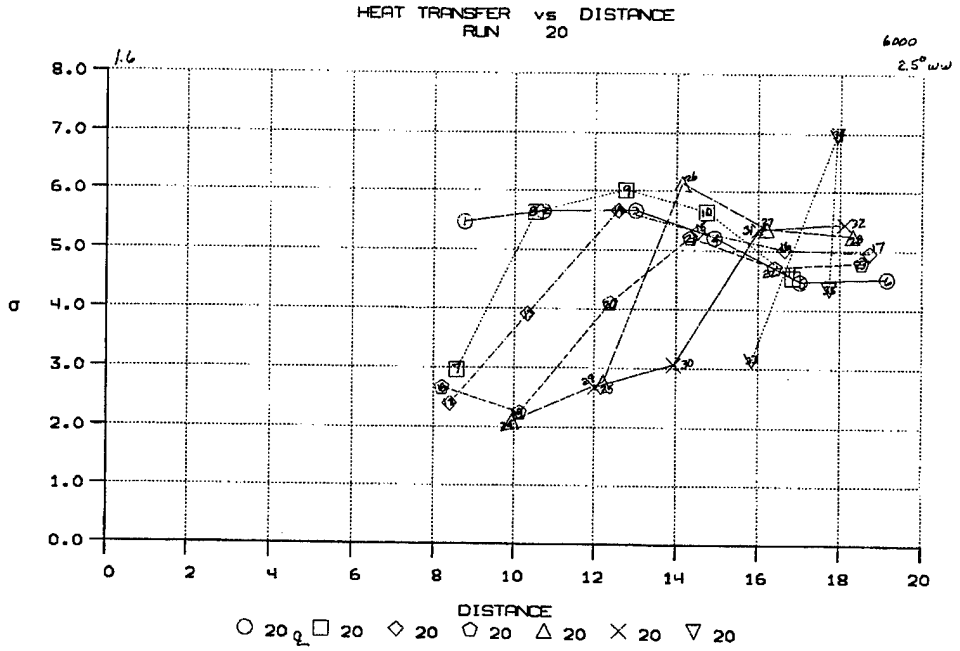

Figure 15a **TYPICAL HEAT TRANSFER MEASUREMENT IN TRANSITIONAL FLOWS OF WINDWARD SURFACE OF ELLIPTIC CONE AT 2.5° INCIDENCE AT LARGE REYNOLDS NUMBER AT MACH 11**

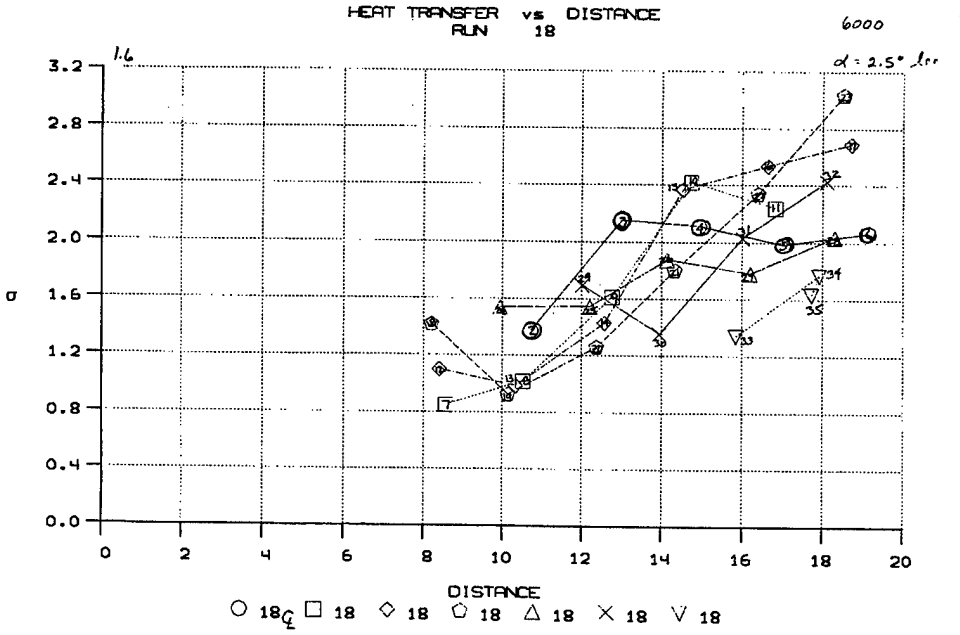

Figure 15b **TYPICAL HEAT TRANSFER MEASUREMENTS IN TRANSITIONAL FLOWS OF LEESIDE SURFACE OF ELLIPTIC CONE AT 2.5° INCIDENCE AT LARGE REYNOLDS NUMBER AT MACH 11**

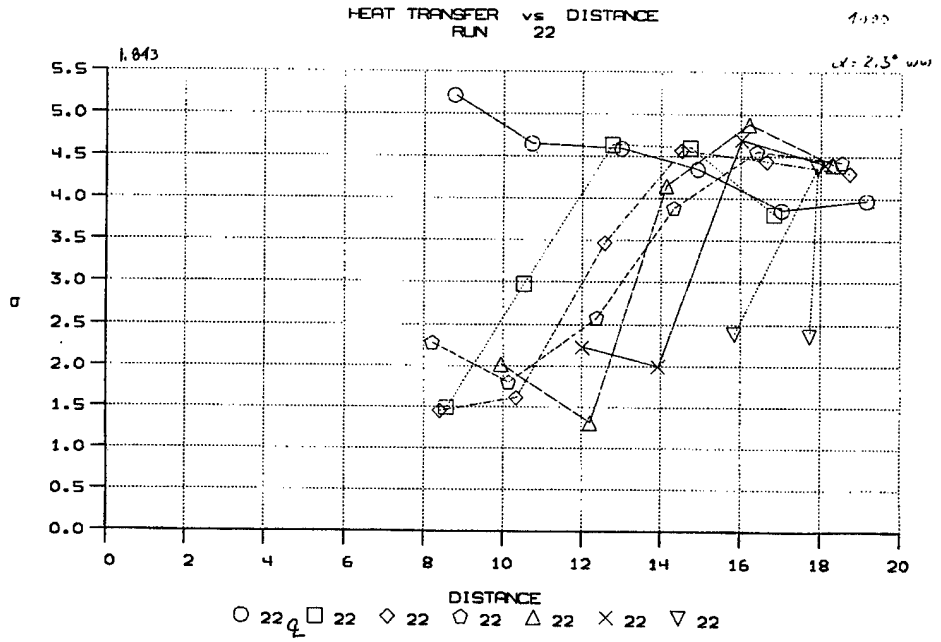

Figure 16a **TYPICAL HEAT TRANSFER MEASUREMENT IN TRANSITIONAL FLOWS ON WINDWARD SURFACE OF ELLIPTIC CONE AT 2.5° INCIDENCE AT MEDIUM REYNOLDS NUMBER AT MACH 11**

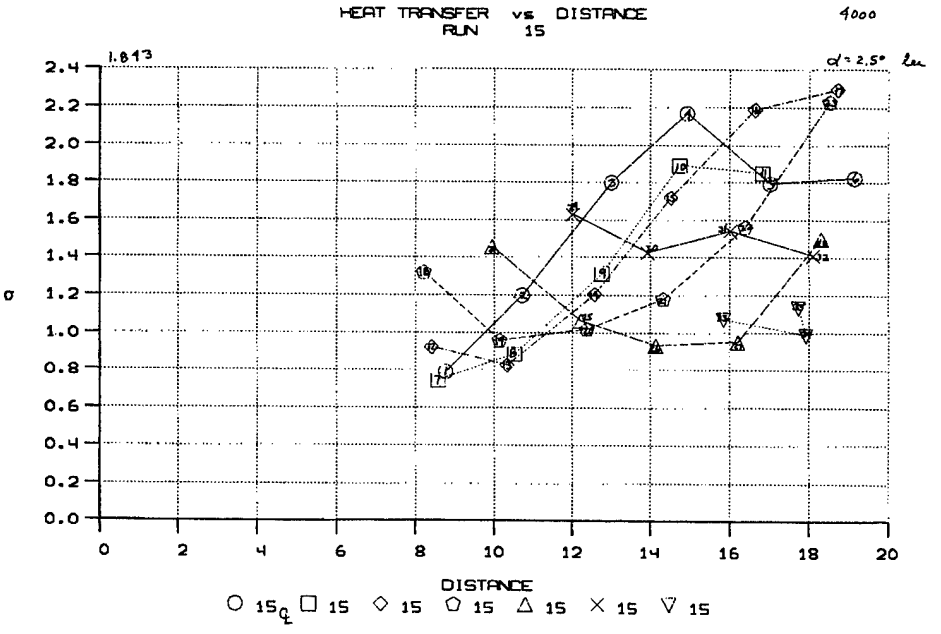

Figure 16b **TYPICAL HEAT TRANSFER MEASUREMENT IN TRANSITIONAL FLOWS ON LEESIDE SURFACE OF ELLIPTIC CONE AT 2.5° INCIDENCE OF MEDIUM REYNOLDS NUMBER AT MACH 11**

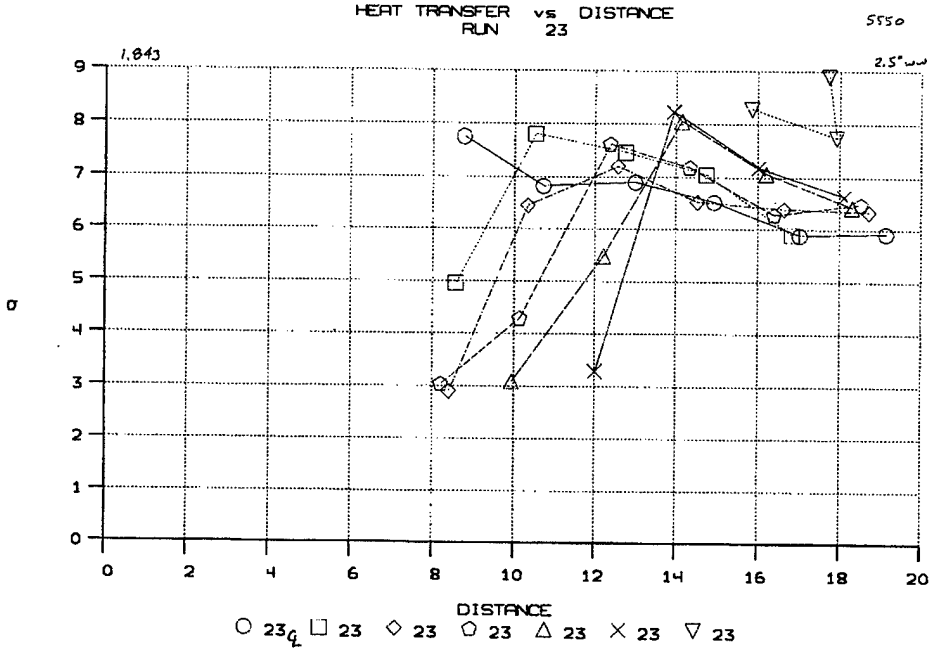

Figure 17a **TYPICAL HEAT TRANSFER MEASUREMENTS IN TRANSITIONAL FLOW ON WINDWARD SURFACE OF ELLIPTIC CONE AT 2.5° INCIDENCE AT HIGH REYNOLDS NUMBER AT MACH 11**

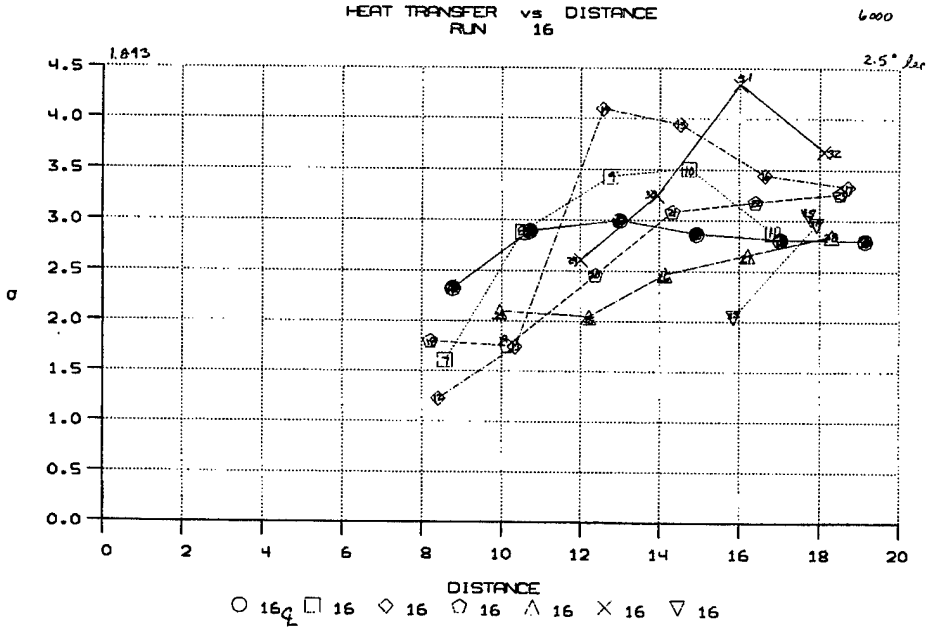

Figure 17b **TYPICAL HEAT TRANSFER MEASUREMENT IN TRANSITIONAL FLOW ON LEESIDE SURFACE OF ELLIPTIC CONE AT 2.5° INCIDENCE AT HIGH REYNOLDS NUMBER AT MACH 11**

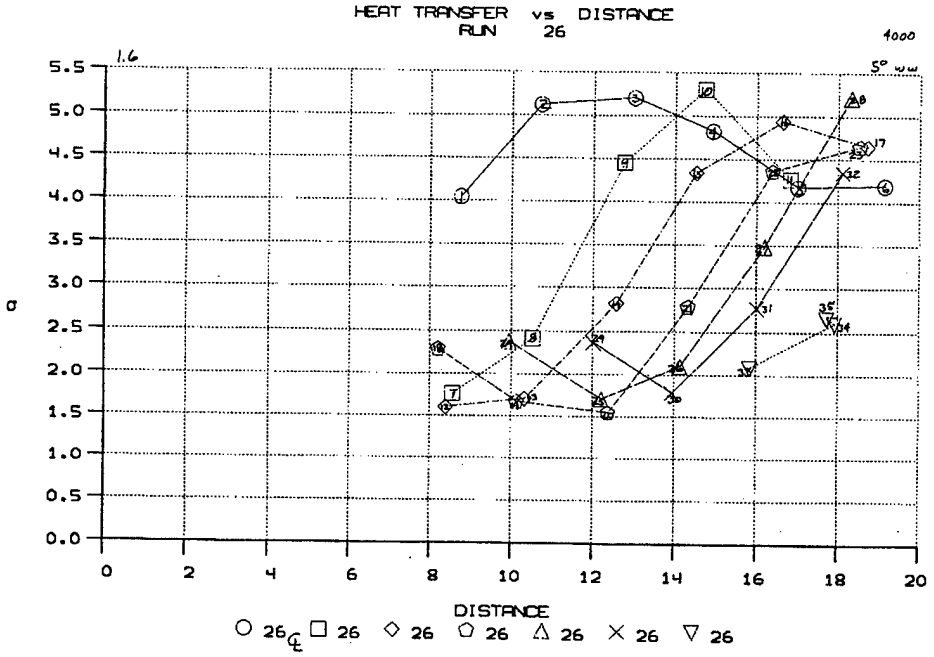

Figure 18a **TYPICAL HEAT TRANSFER MEASUREMENTS ON LEESIDE SURFACE OF ELLIPTIC CONE AT 5° ANGLE OF ATTACK AT MEDIUM REYNOLDS NUMBER AT MACH 11**

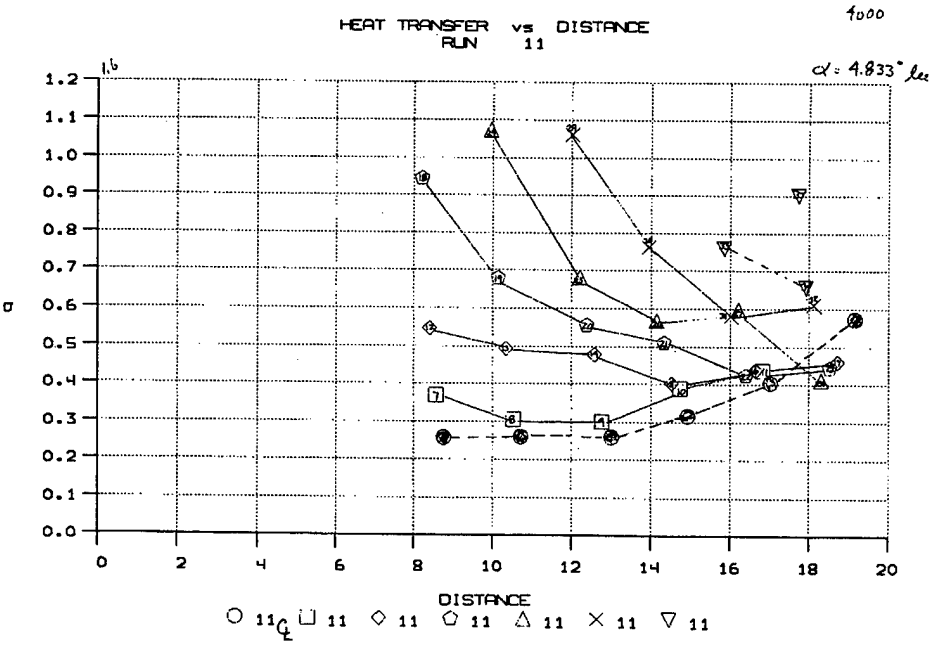

Figure 18b **TYPICAL HEAT TRANSFER MEASUREMENTS ON LEESIDE SURFACE OF ELLIPTIC CONE AT 5° ANGLE OF ATTACK AT MEDIUM REYNOLDS NUMBER AT MACH 11**

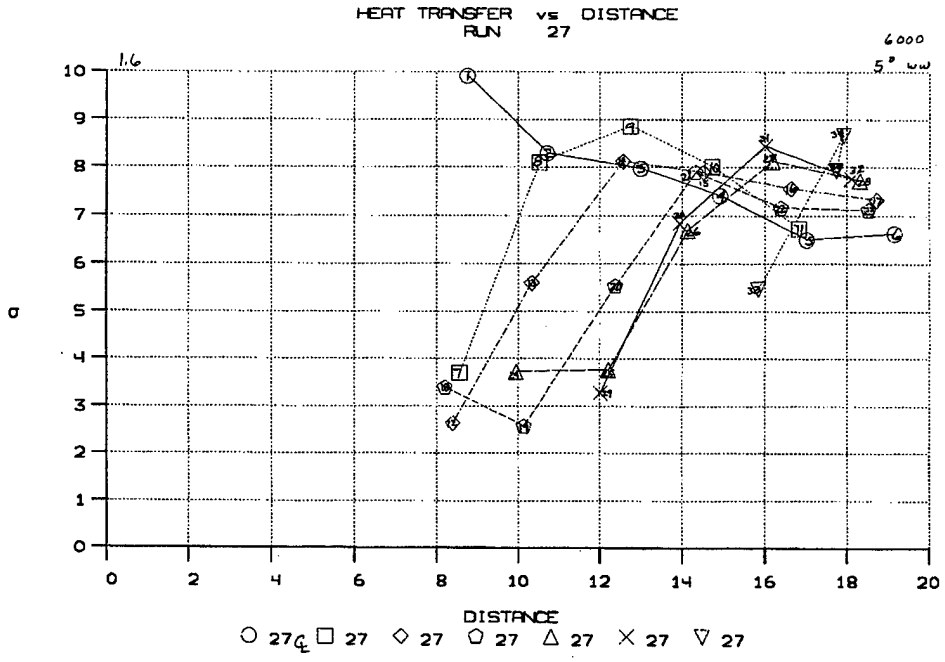

Figure 19a **TYPICAL HEAT TRANSFER MEASUREMENTS ON WINDWARD SURFACE OF ELLIPTIC CONE AT 5° INCIDENCE AT LARGE REYNOLDS NUMBER AT MACH 11**

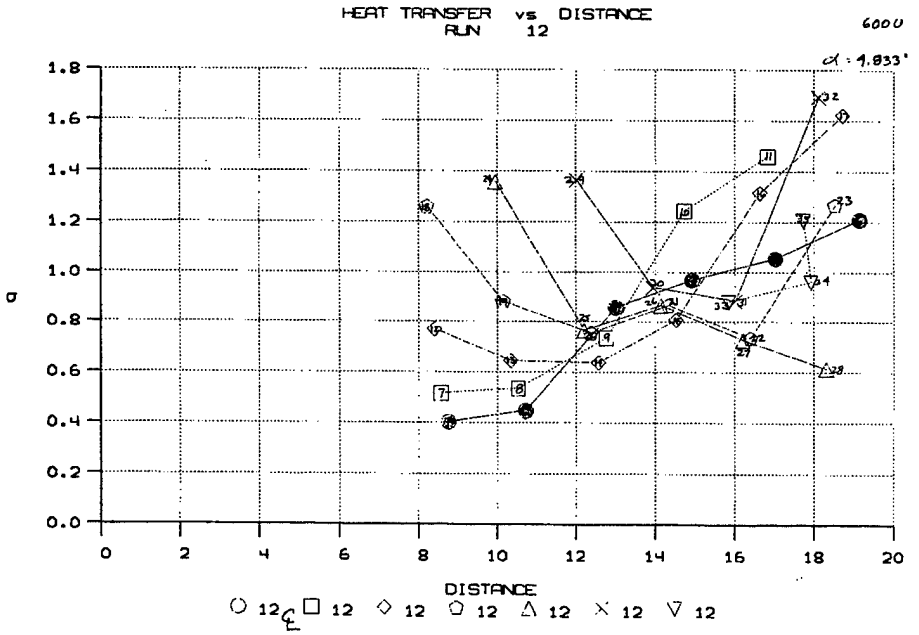

Figure 19b **TYPICAL HEAT TRANSFER MEASUREMENTS ON LEESIDE SURFACE OF ELLIPTIC CONE AT 5° INCIDENCE AT LARGE REYNOLDS NUMBER AT MACH 11**

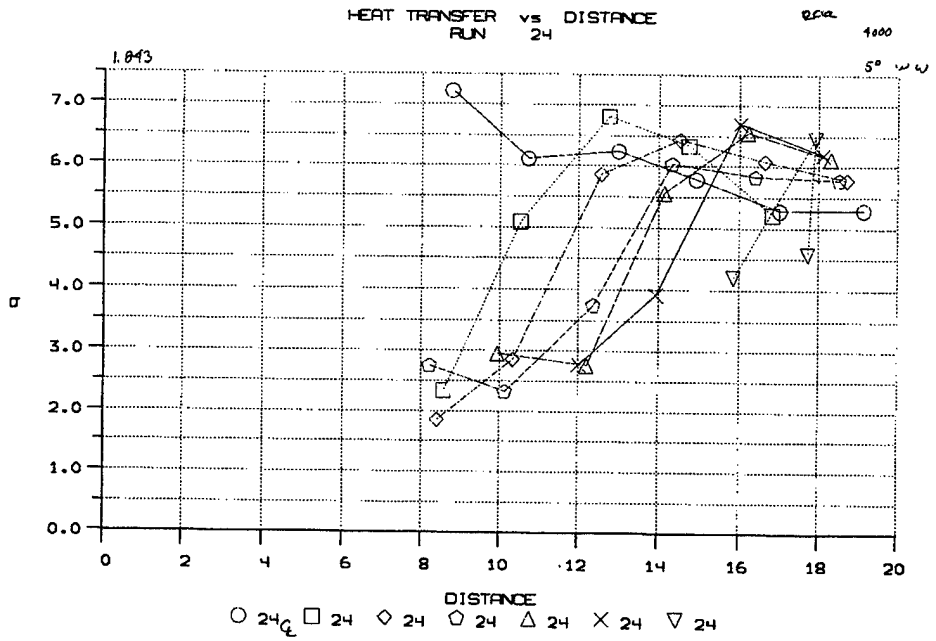

Figure 20a **TYPICAL HEAT TRANSFER RATE IN TRANSITION REGION ON WINDWARD SURFACE OF ELLIPTIC CONE AT 5° INCIDENCE AT MEDIUM REYNOLDS NUMBER AT MACH 11**

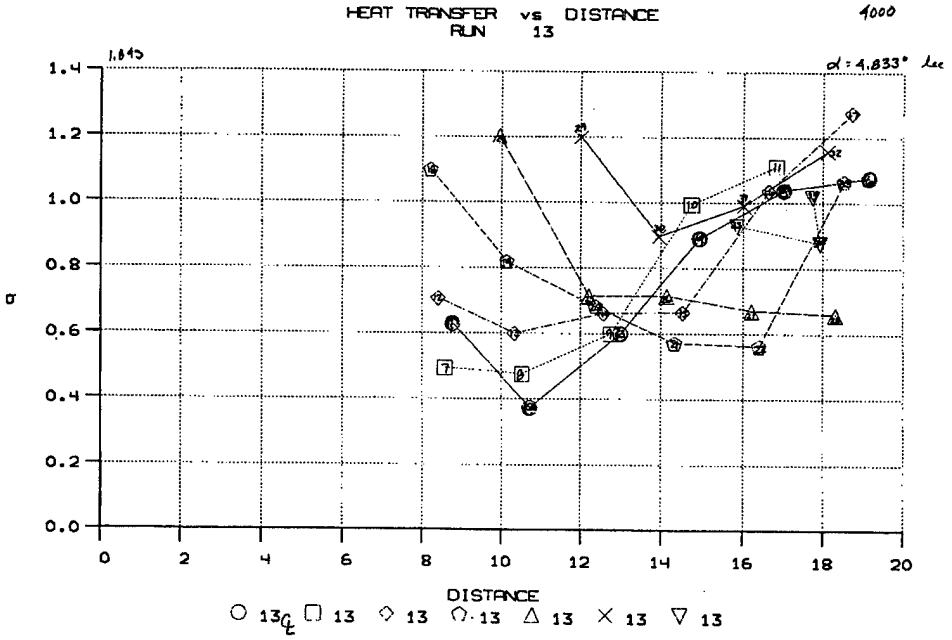

Figure 20b **TYPICAL HEAT TRANSFER RATE IN TRANSITION REGION ON LEESIDE SURFACE OF ELLIPTIC CONE AT 5° INCIDENCE AT MEDIUM REYNOLDS NUMBER AT MACH 11**

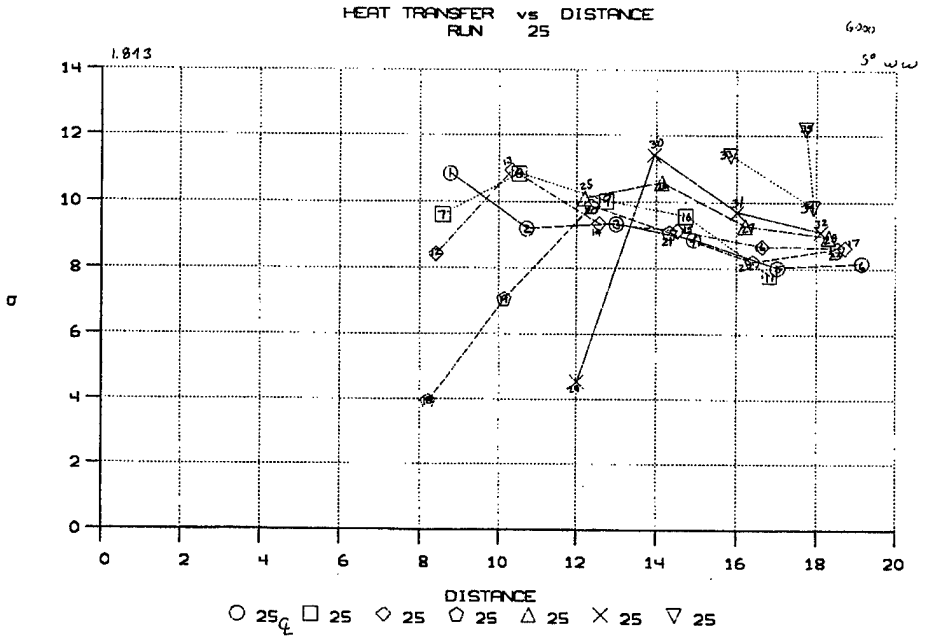

Figure 21a **TYPICAL HEAT TRANSFER ON WINDWARD RAY OF ELLIPTIC CONE AT 5° INCIDENCE AT HIGH REYNOLDS NUMBER AT MACH 8**

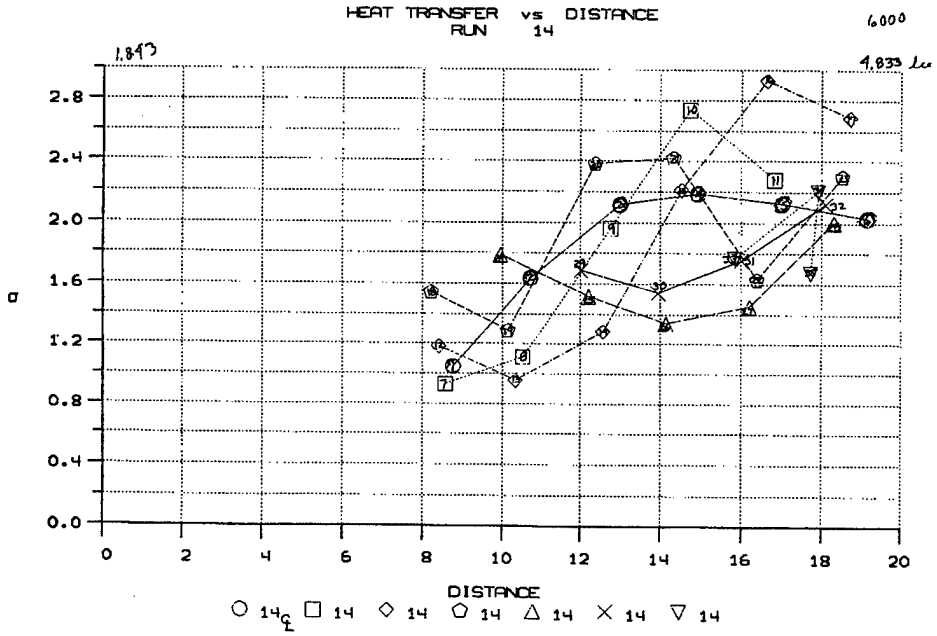

Figure 21b **TYPICAL HEAT TRANSFER ON LEESIDE RAY OF ELLIPTIC CONE AT 5° INCIDENCE AT HIGH REYNOLDS NUMBER AT MACH 8**

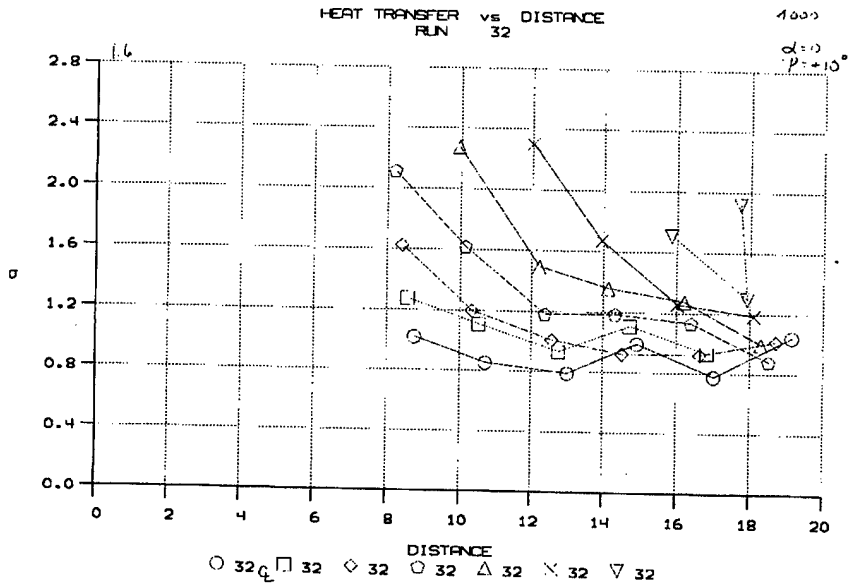

Figure 22a **TYPICAL HEAT TRANSFER MEASUREMENTS ON ELLIPTIC CONE YAWED AT +10° AT MEDIUM REYNOLDS NUMBER AT MACH 8**

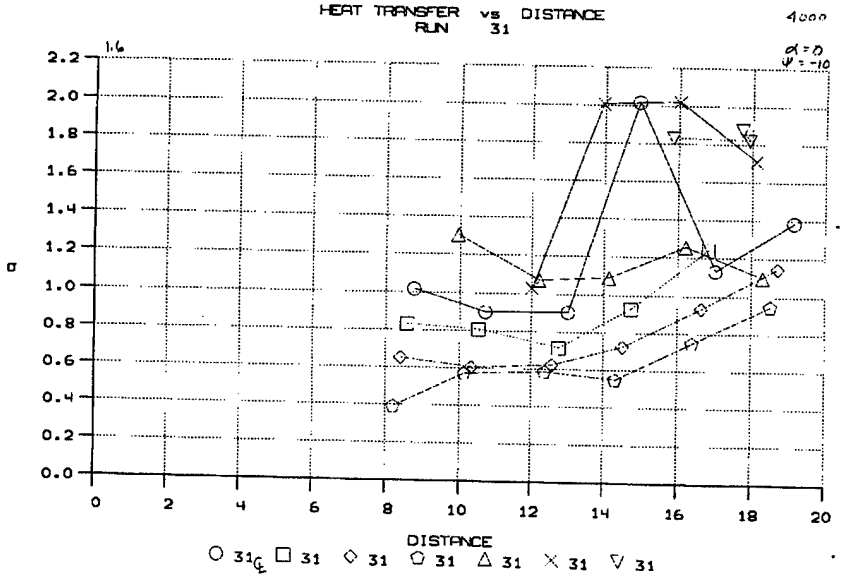

Figure 22b **TYPICAL HEAT TRANSFER MEASUREMENTS IN TRANSITIONAL FLOW OVER AN ELLIPTIC CONE YAWED AT –10° AT MEDIUM REYNOLDS NUMBER AT MACH 8**

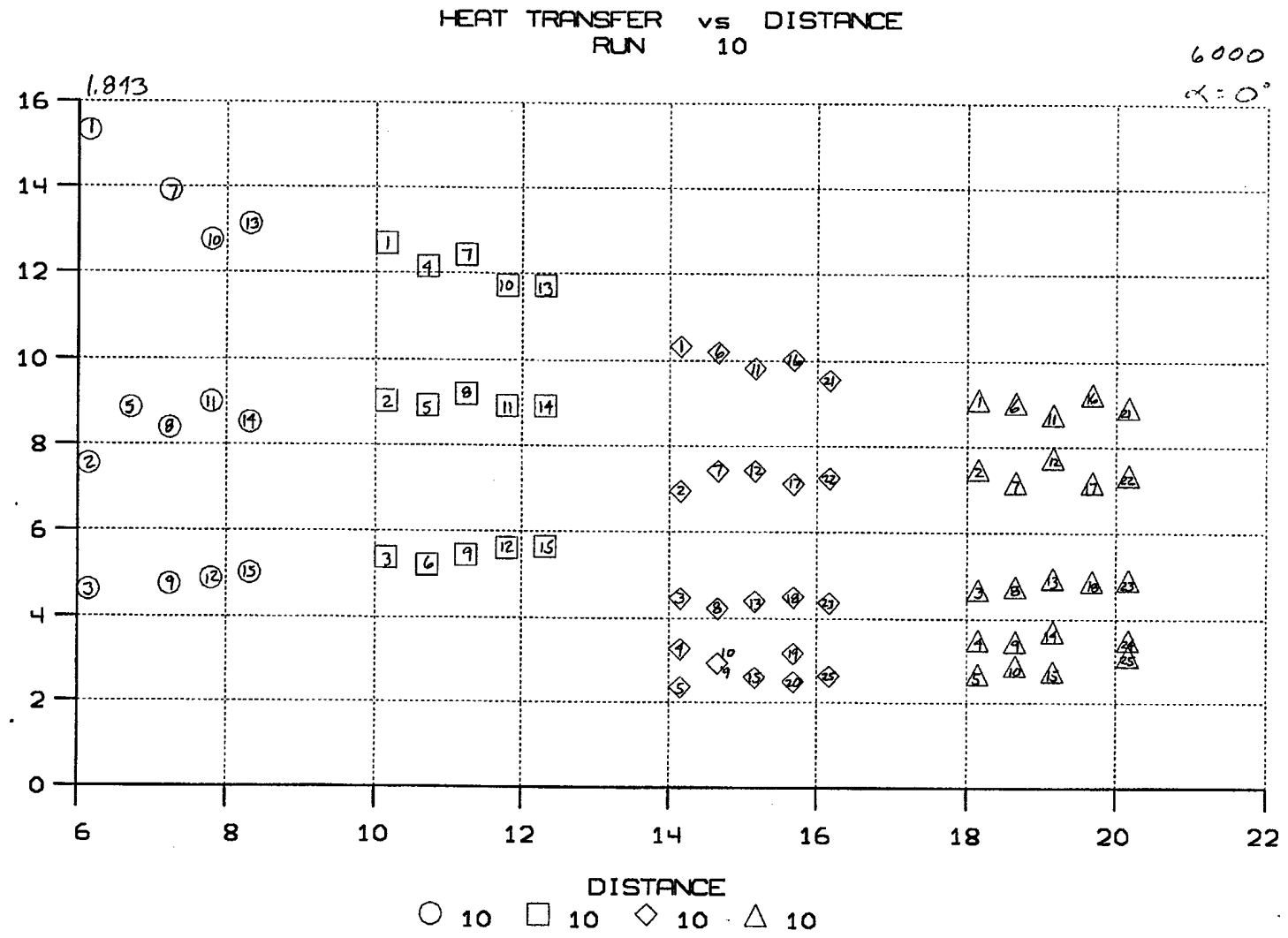

Figure 23 **HEAT TRANSFER MEASUREMENT ON LEADING EDGE OF ELLIPTIC CONE AT HIGH REYNOLDS NUMBER AT MACH 8**

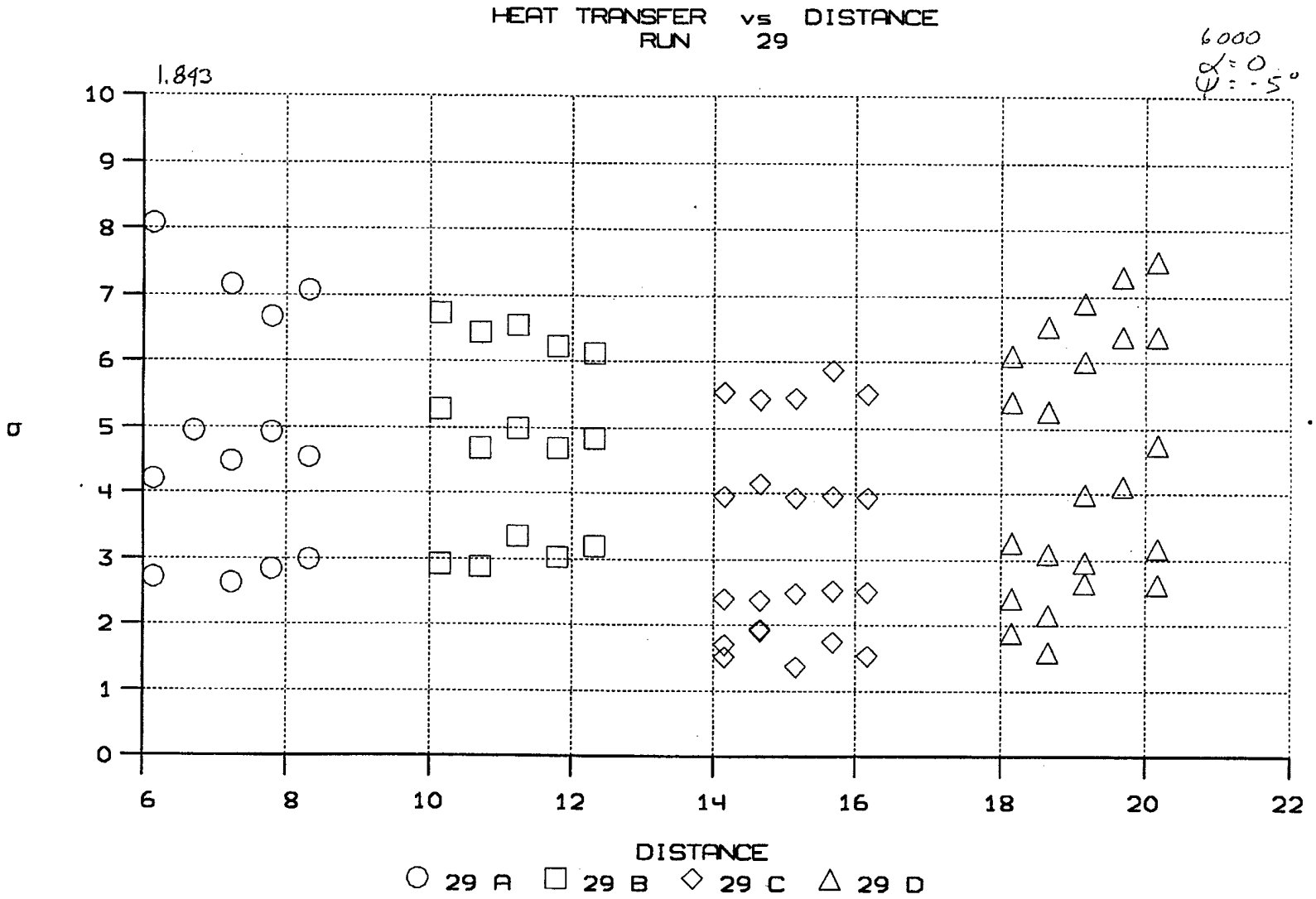

Figure 24 **HEAT TRANSFER MEASUREMENT ON LEADING EDGE OF ELLIPTIC CONE YAWED AT –5° YAW AT HIGH REYNOLDS NUMBER AT MACH 8**

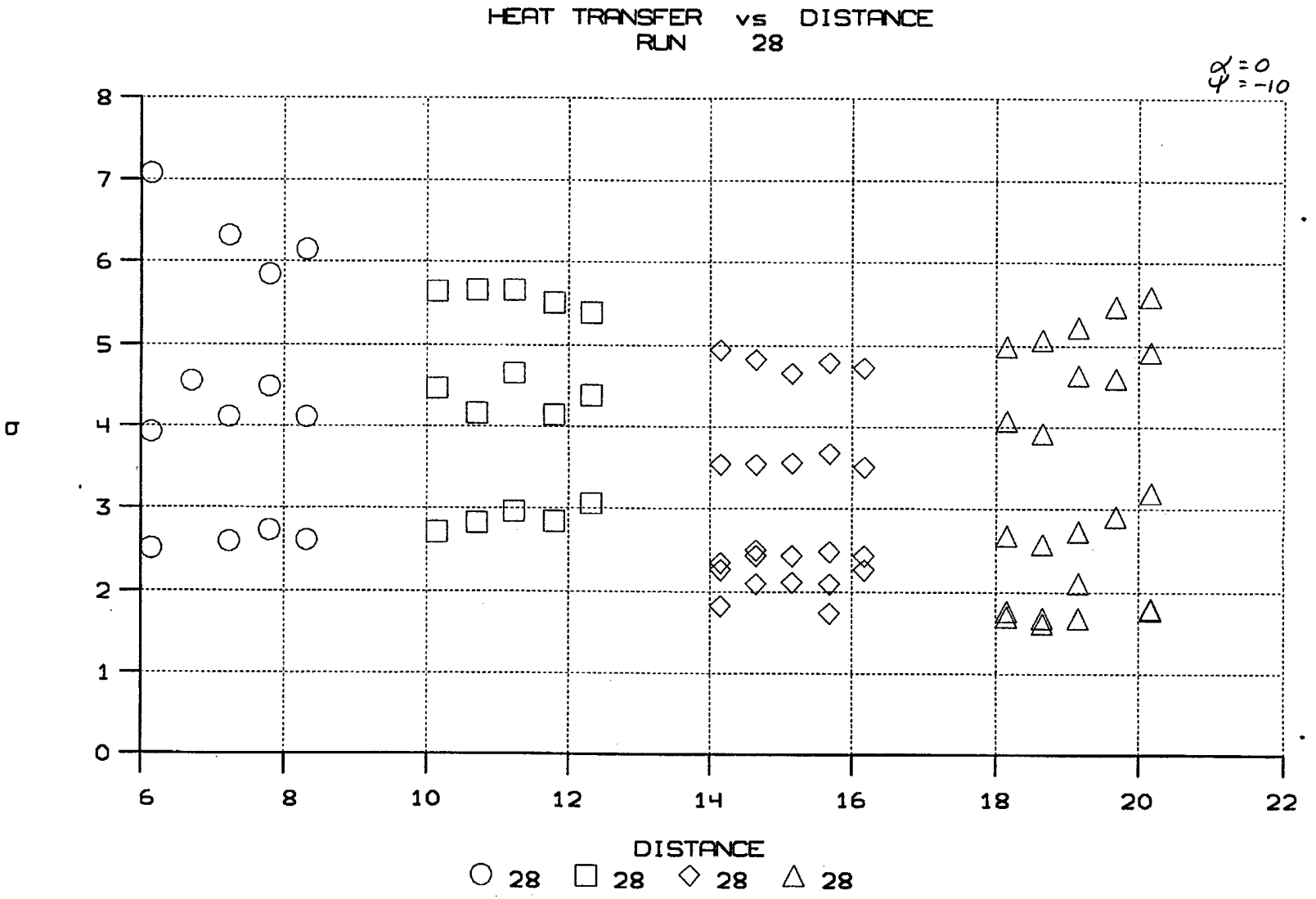

Figure 25 **HEAT TRANSFER MEASUREMETNS ON LEADING EDGE OF ELLIPTIC CONE YAWED AT –10° YAW AT HIGH REYNOLDS NUMBER AT MACH 8**

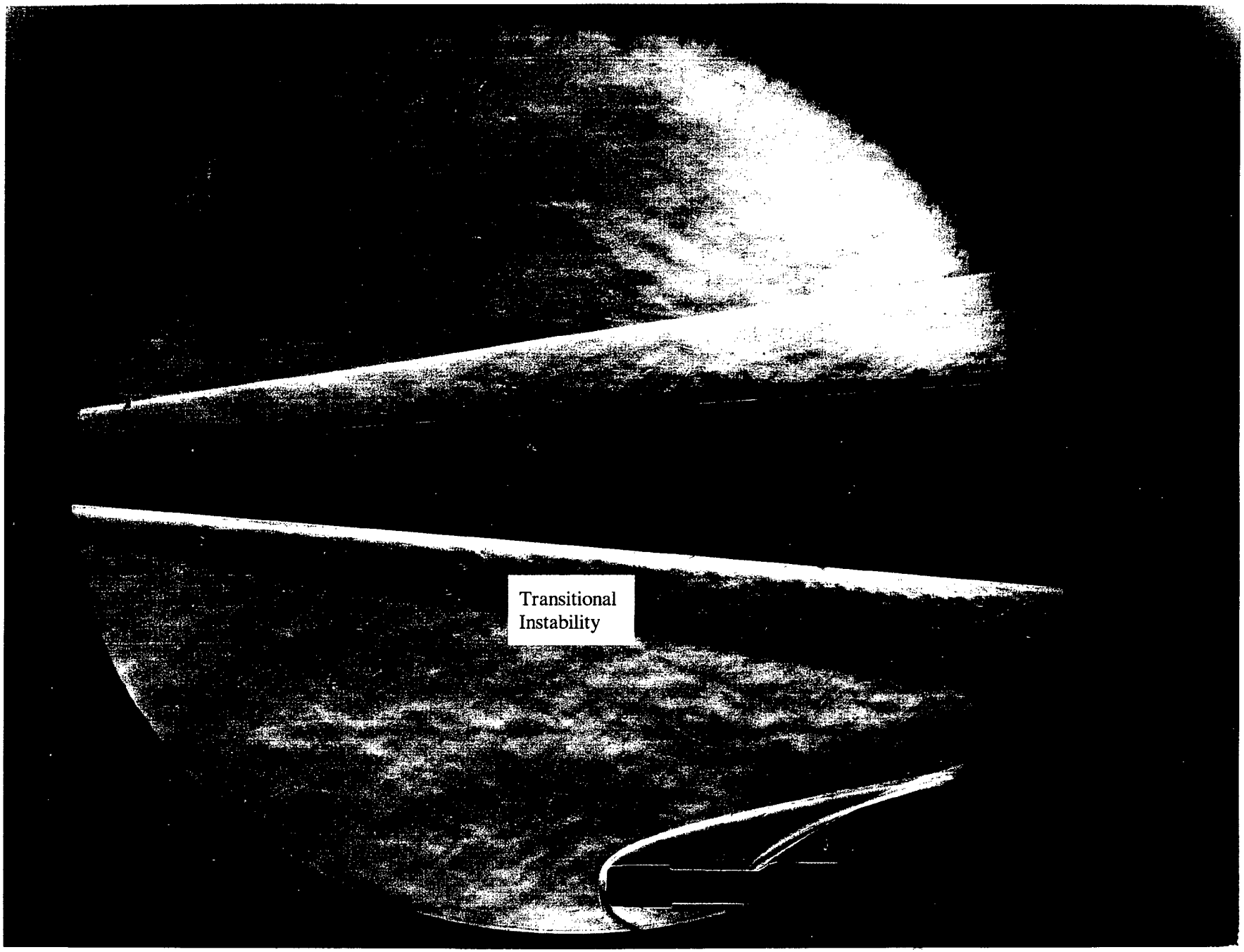

Figure 26 **SCHLIEREN PHOTOGRAPH OF TRANSITIONAL FLOW INSTABILITIES AND TRANSITION FLOW REGION AT MACH 11 FOR MODEL AT 0° INCIDENCE**

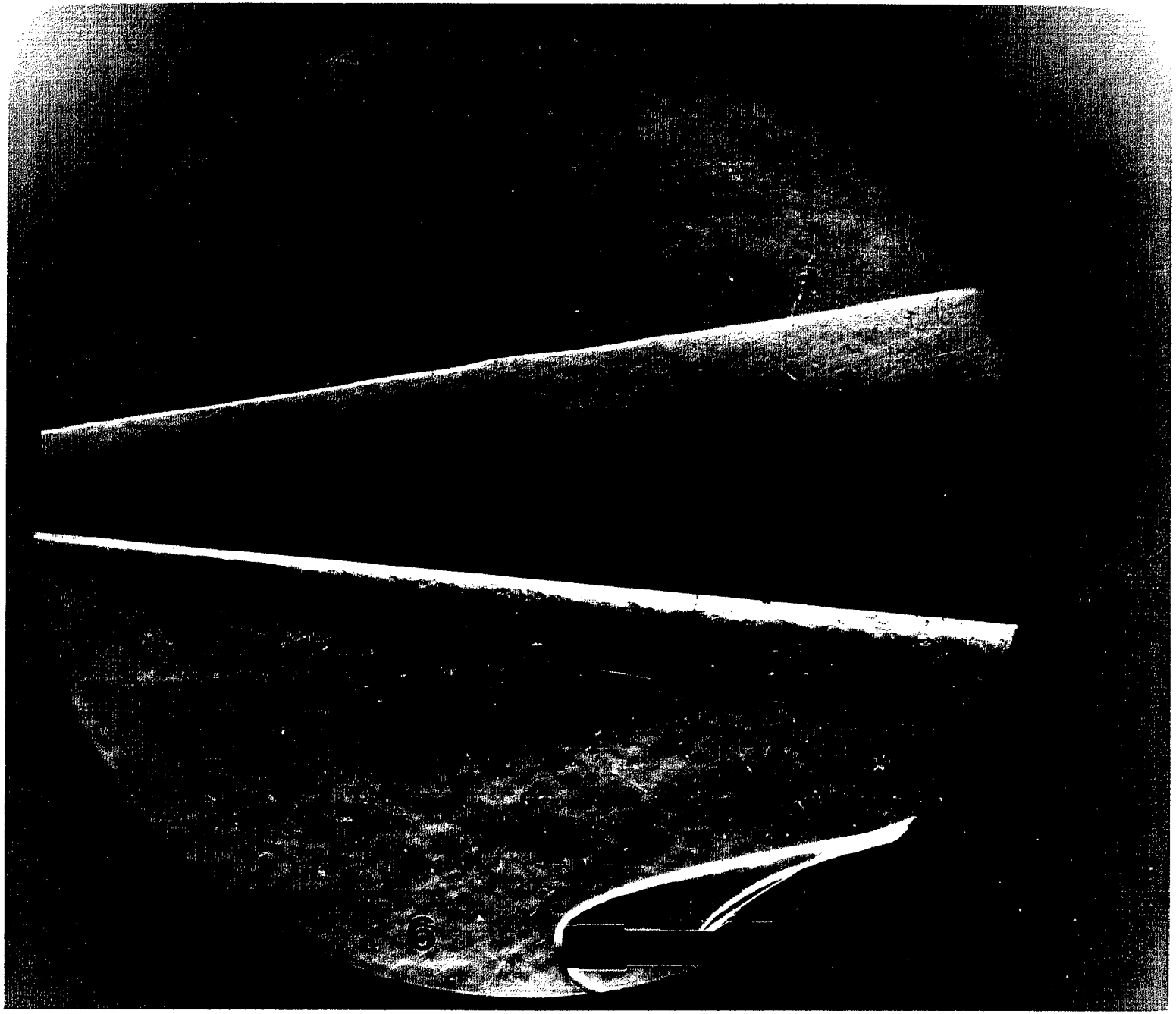

Figure 27 **TYPICAL EXAMPLE OF TRANSITIONAL FLOW STRUCTURE ON ELLIPTIC CONE AT 0°INCIDENCE AT MACH 11**

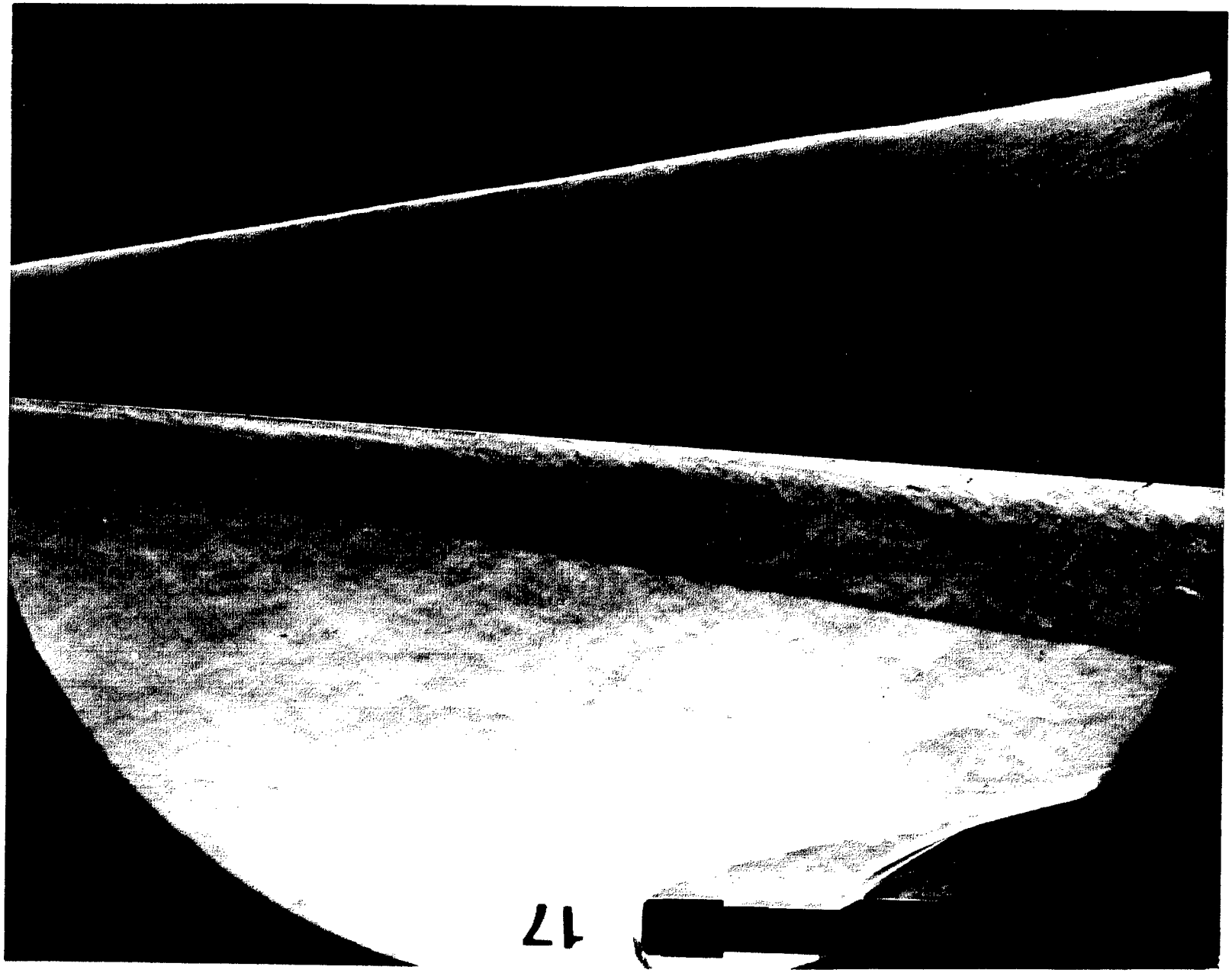

Figure 28 **TYPICAL SCHLIEREN PHOTOGRAPH OF TRANSITIONAL FLOW OVER ELLIPTIC CONE AT 5° INCIDENCE**

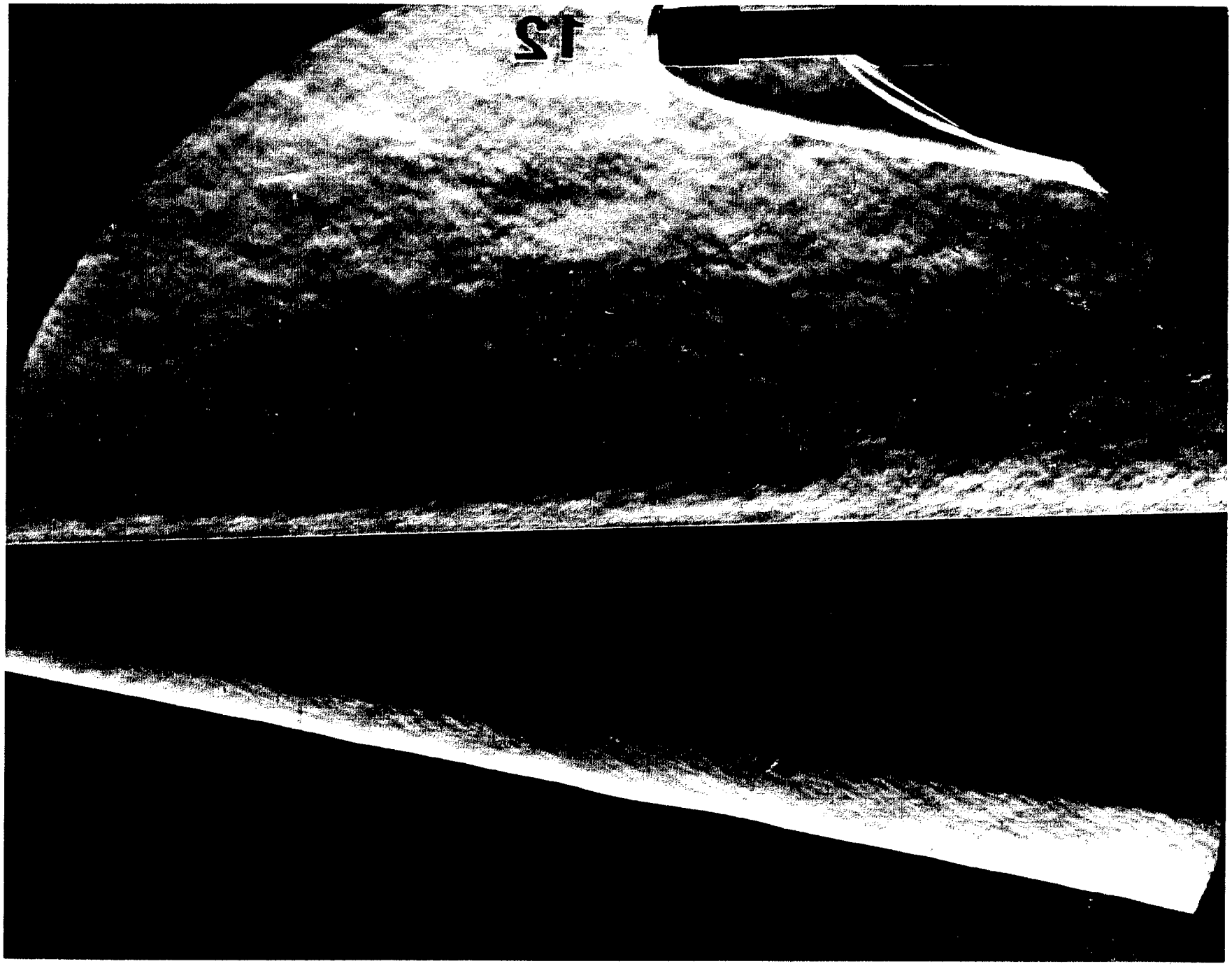

Figure 29 **TYPICAL SCHLIEREN PHOTOGRAPH OF TRANSITIONAL FLOW OVER ELLIPTIC CONE AT 2.5° INCIDENCE**

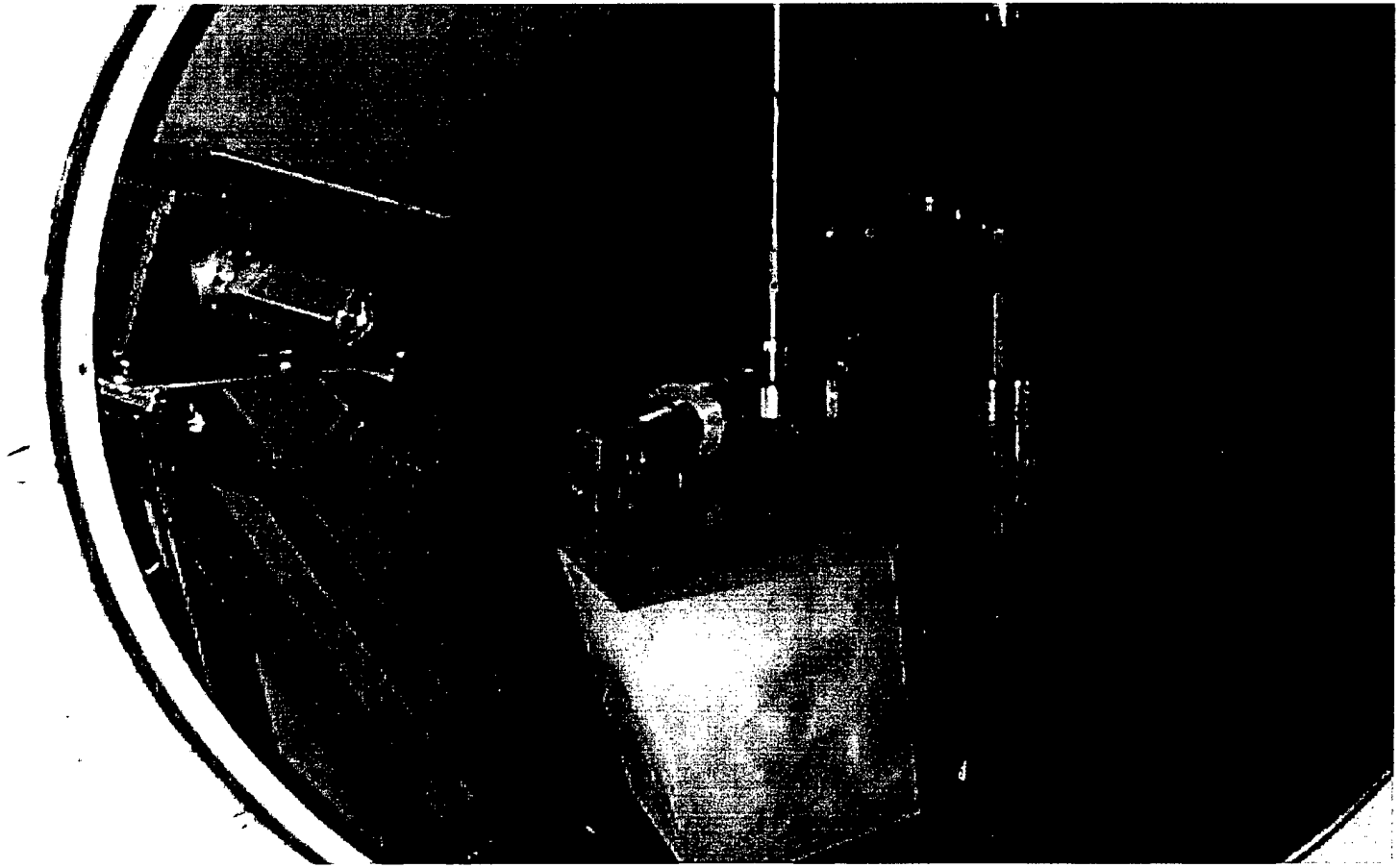

Figure 30 ELECTRON BEAM INSTALLED IN LENS FACILITY

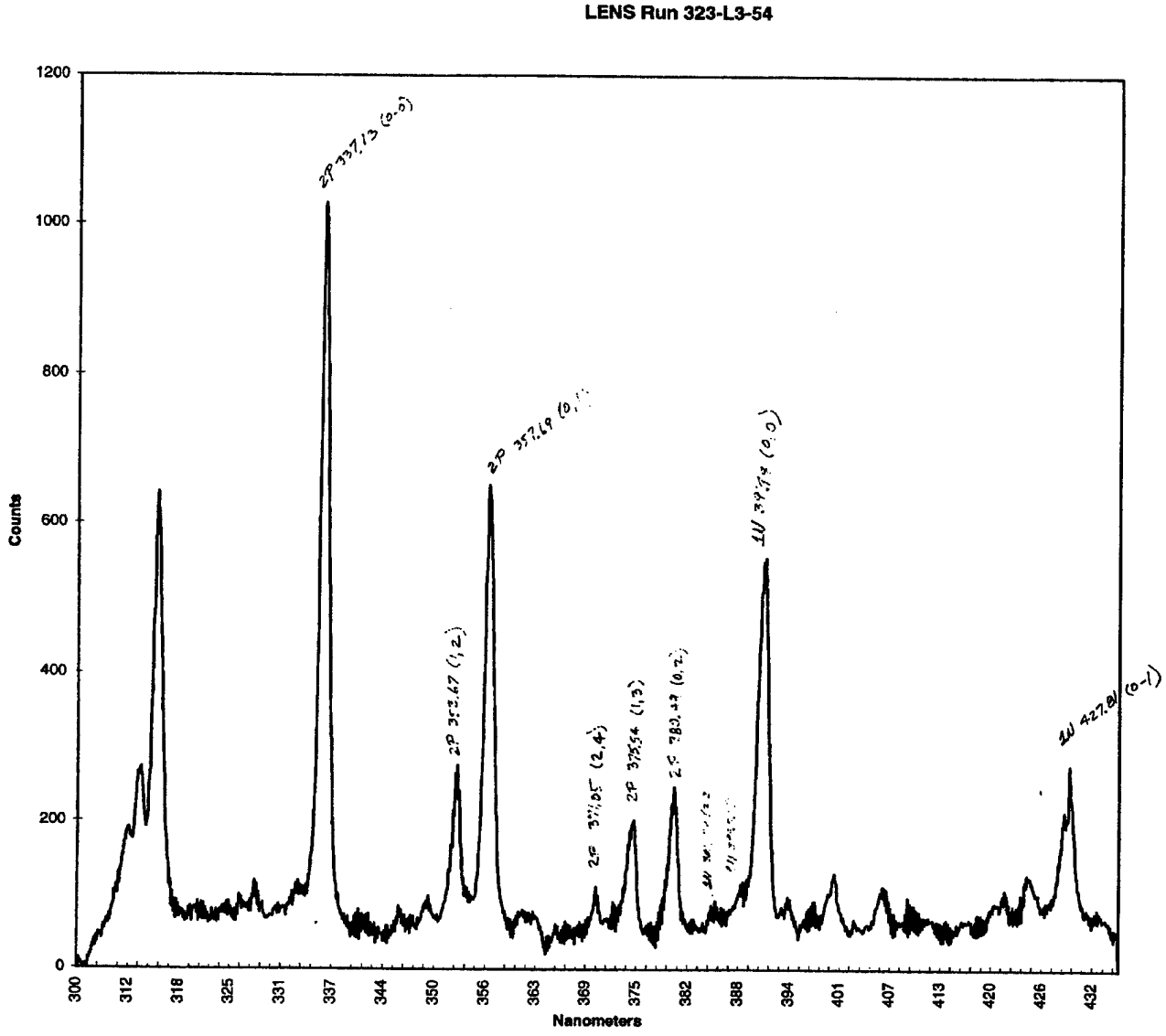

Figure 31 N_2 **SPECTRA FROM ELECTRON BEAM STUDIES**

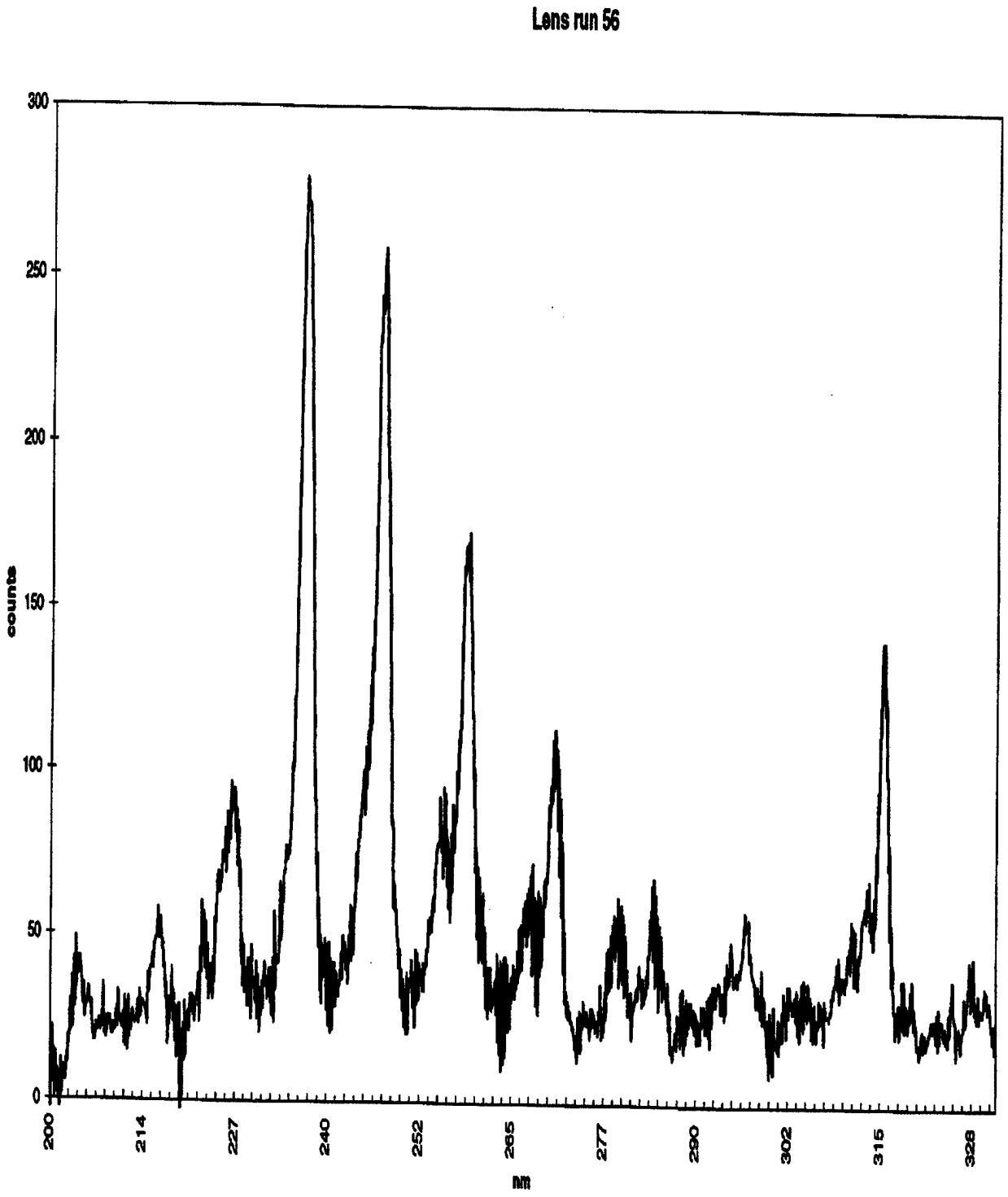

Figure 32 NO SPECTRA FROM ELECTRON BEAM APPARATUS

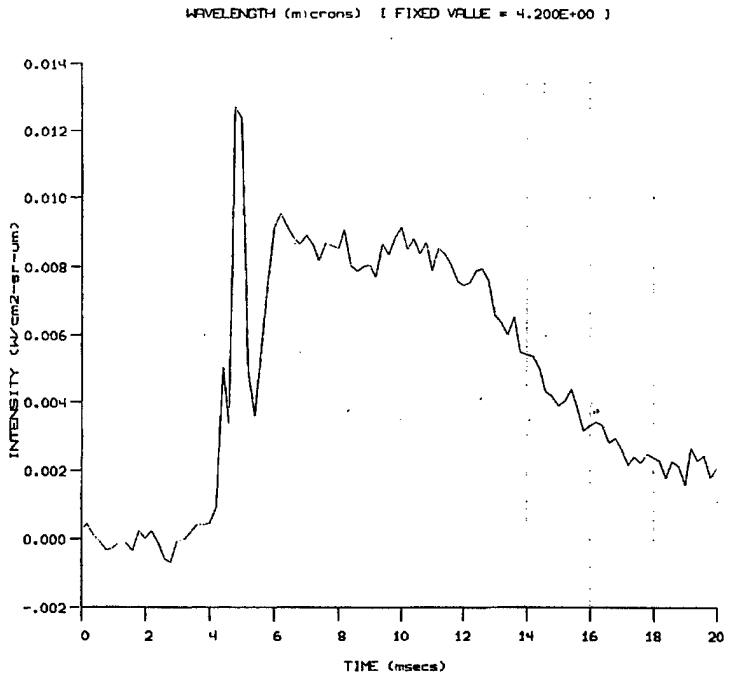

Figure 33a CO_2 RADIATION SIGNAL TIME HISTORY

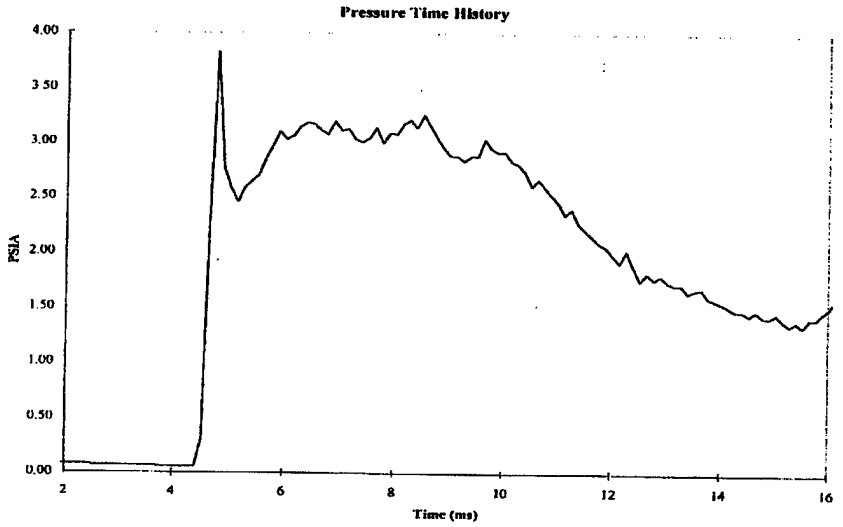

Figure 33b PITOT PRESSURE MEASUREMENT TIME